AGU PUBLICATIONS

Reviews of Geophysics

REVIEW ARTICLE
10.1002/2017RG000568

Key Points:
- The character of ENSO as well as the ocean mean state has changed since the 1990s, resulting in changes in ENSO atmospheric teleconnections
- Changes in ENSO teleconnection patterns have affected their predictability and the statistics of extreme events
- Climate models suggest that changes in the mean atmospheric circulation will affect ENSO teleconnections in the 21st century

Correspondence to:
S.-W. Yeh,
swyeh@hanyang.ac.kr

Citation:
Yeh, S.-W., Cai, W., Min, S.-K., McPhaden, M. J., Dommenget, D., Dewitte, B., … Kug, J.-S. (2018). ENSO atmospheric teleconnections and their response to greenhouse gas forcing. *Reviews of Geophysics*, *56*, 185–206. https://doi.org/10.1002/2017RG000568

Received 18 APR 2017
Accepted 10 JAN 2018
Accepted article online 15 JAN 2018
Published online 17 FEB 2018
Corrected 17 AUG 2018

This article was corrected on 17 AUG 2018. See the end of the full text for details.

ENSO Atmospheric Teleconnections and Their Response to Greenhouse Gas Forcing

Sang-Wook Yeh[1], Wenju Cai[2,3], Seung-Ki Min[4], Michael J. McPhaden[5], Dietmar Dommenget[6], Boris Dewitte[7,8], Matthew Collins[9], Karumuri Ashok[10], Soon-Il An[11], Bo-Young Yim[12], and Jong-Seong Kug[4]

[1]Department of Marine Science and Convergent Technology, Hanyang University, Ansan, Korea, [2]Centre for Southern Hemisphere Oceans Research, CSIRO, Hobart, Tasmanina, Australia, [3]Physical Oceanography Laboratory/CIMSST, Ocean University of China and Qingdao National Laboratory for Marine Science and Technology, Qingdao, China, [4]Devision of Environmental Science and Engineering, Pohang University of Science and Technology, Pohang, Korea, USA, [5]NOAA/Pacific Marine Environmental Laboratory, Seattle, WA, USA, [6]School of Earth, Atmosphere and Environment, Monash University, Clayton, Victoria, Australia, [7]Centro de Estudios Avanzado en Zonas Áridas, Coquimbo, Chile, [8]Laboratoire d'Etudes en Géophysique et Océanographie Spatiales, Toulouse, France, [9]College of Engineering Mathematics and Physical Sciences, University of Exeter, Exeter, UK, [10]Centre for Earth and Space Sciences (UCESS), University of Hyderabad, Hyderabad, India, [11]Department of Atmospheric Science, Yonsei University, Seoul, Korea, [12]Korea Meteorological Administration, Seoul, Korea

Abstract El Niño and Southern Oscillation (ENSO) is the most prominent year-to-year climate fluctuation on Earth, alternating between anomalously warm (El Niño) and cold (La Niña) sea surface temperature (SST) conditions in the tropical Pacific. ENSO exerts its impacts on remote regions of the globe through atmospheric teleconnections, affecting extreme weather events worldwide. However, these teleconnections are inherently nonlinear and sensitive to ENSO SST anomaly patterns and amplitudes. In addition, teleconnections are modulated by variability in the oceanic and atmopsheric mean state outside the tropics and by land and sea ice extent. The character of ENSO as well as the ocean mean state have changed since the 1990s, which might be due to either natural variability or anthropogenic forcing, or their combined influences. This has resulted in changes in ENSO atmospheric teleconnections in terms of precipitation and temperature in various parts of the globe. In addition, changes in ENSO teleconnection patterns have affected their predictability and the statistics of extreme events. However, the short observational record does not allow us to clearly distinguish which changes are robust and which are not. Climate models suggest that ENSO teleconnections will change because the mean atmospheric circulation will change due to anthropogenic forcing in the 21st century, which is independent of whether ENSO properties change or not. However, future ENSO teleconnection changes do not currently show strong intermodel agreement from region to region, highlighting the importance of identifying factors that affect uncertainty in future model projections.

1. Introduction

The El Niño and Southern Oscillation (ENSO) is the most prominent mode of interannual climate variability on Earth. It is generated through coupled interactions between the ocean and atmosphere in the tropical Pacific (Bjerknes, 1969) and alternates between anomalously warm (El Niño) and cold (La Niña) sea surface temperature (SST) conditions. Figure 1 displays a schematic diagram showing the tropical weather and oceanic condition along the equator during normal, El Niño and La Niña conditions. During El Niño, the surface air pressure over the tropical western Pacific becomes higher than in the tropical eastern tropical Pacific compared to a normal year, resulting in weaker trade winds and surface zonal currents. The prevailing rain pattern also shifts further east than normal. Weaker trade winds act to reduce ocean upwelling intensity, leading to a deeper thermocline and warmer-than-normal SSTs in the eastern and central tropical Pacific. During La Niña, in contrast, the trade winds in the tropical Pacific basin are stronger than normal, leading to the increase of the upwelling intensity off South America and along the equator and hence the lower than normal SSTs. The center of the prevailing rain pattern also shifts farther west than normal during La Niña.

ENSO has enormous impacts on natural and human systems including agriculture, forestry, public health, the hydrological cycle, the global carbon cycle, marine and terrestrial ecosystems, and fisheries (McPhaden et al., 2006). The impacts on regions outside the tropical Pacific arise through atmospheric teleconnections (Bjerknes, 1969; Diaz et al., 2001; Horel & Wallace, 1981; McPhaden et al., 2006; Stan et al., 2017; Trenberth et al., 1998)

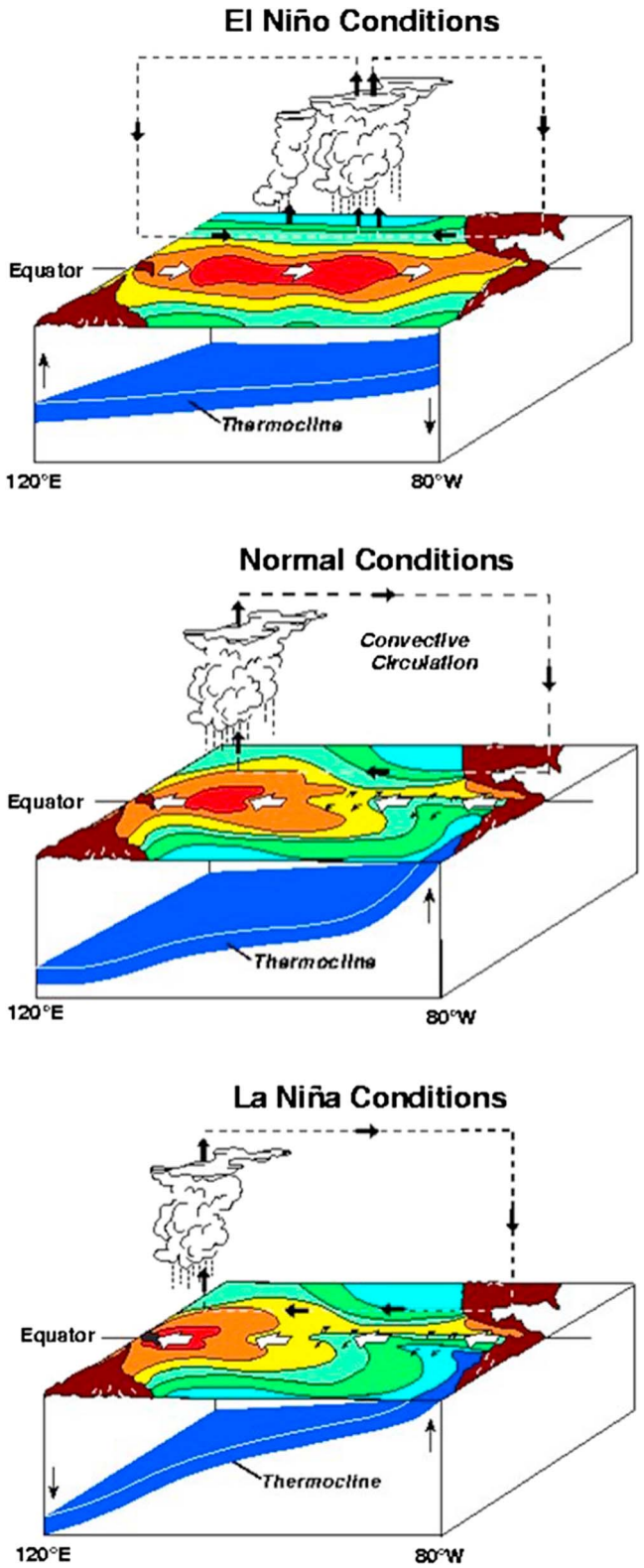

Figure 1. Schematic diagrams showing the tropical weather and oceanic condition across the equator during canonical El Niño (upper) and canonical La Niña (lower). Figure courtesy of the Pacific Marine Environmental Laboratory/National Oceanic and Atmospheric Administration.

and oceanic teleconnections (England & Huang, 2005; Feng et al., 2013; Frischknecht et al., 2015; Gordon & Fine, 1996; Hazeleger et al., 2004; McPhaden et al., 2006; Vergara et al., 2017). The term "teleconnection" refers to a statistically significant remote response, either concurrent with or time lagged, from a forcing region, which in the case of ENSO is the equatorial Pacific.

ENSO oceanic teleconnections include, for example, heat extremes off the west coast of Australia via the Indonesian Throughflow (Feng et al., 2013). Equatorial wind anomalies associated with ENSO also generate oceanic Kelvin waves along the west coast of the Americas (Clarke & van Gorder, 1994), affecting coastal marine ecosystems and fisheries (Gutierrez et al., 2008; Meyers et al., 1998). In addition, the anomalous poleward oceanic heat transport following El Niño and La Niña events can affect the heat budget of the high-latitude oceans and hence the tropical cyclone activity (Gordon & Fine, 1996; Jin et al., 2014). ENSO atmospheric teleconnections have a strong and broad impact on global climate and weather events, and it is on these teleconnections that we focus this review.

During the mature phase of El Niño, the heat source in the tropical western Pacific expands eastward (Sikka, 1980; Wang, 2002). This eastward movement weakens the Pacific Walker circulation that in turn weakens the lower-tropospheric equatorial easterly trade winds. The reverse occurs during the mature phase of La Niña. Through the tropical atmospheric bridge via modulation of the Walker circulation (i.e., the near-equatorial zonal atmospheric overturning circulation), ENSO atmospheric teleconnections induce changes in cloud cover and evaporation in remote ocean basins such as the South China Sea, the Indian Ocean, and the tropical North Atlantic, with a time lag of 3 to 6 months (Klein et al., 1999; Wang, 2002). For example, during a developing period of El Niño, together with the eastward migration of the prevailing atmospheric convection over the tropical Pacific, the Walker circulation moves to the east, resulting in anomalous atmospheric subsidence over the Indian Ocean region and consequent suppression of convection there. This leads to warming in the Indian Ocean through intensified solar radiation as well as a weakening land-sea contrast in summer, resulting in less Indian summer monsoon rainfall. The opposite happens during La Niña (Webster et al., 1998). During boreal springs after the peak of El Niño events, the northeast trade winds usually weaken and the SST increases over the northern tropical Atlantic Ocean, which is associated with an atmospheric wave train generated in the central tropical Pacific (Huang, 2004).

ENSO atmospheric teleconnections also influence weather and climate conditions over other parts of the globe (Alexander et al., 2002; Chiodi & Harrison, 2015; Deser, 2000; Lau, 1997; Trenberth et al., 1998). Changes in deep convection due to ENSO leads to the changes in atmospheric heating, low-level convergence, and upper-level divergence in the equatorial Pacific (Figure 2; see also Hoskins & Karoly, 1981). The anomalous horizontal component of upper-level atmospheric vorticity forces large-scale atmospheric Rossby waves that propagate into the extratropics (Hoskins & Karoly, 1981; Trenberth et al., 1998) to excite a "Pacific-North American (PNA)" pattern (Horel & Wallace, 1981) (Figures 2a and 2b) and "Pacific-South American (PSA)" pattern (Karoly, 1989) (Figures 2e and 2f) in the Northern and Southern Hemispheres, respectively. These teleconnections influence weather and climate, including extreme events, around the globe.

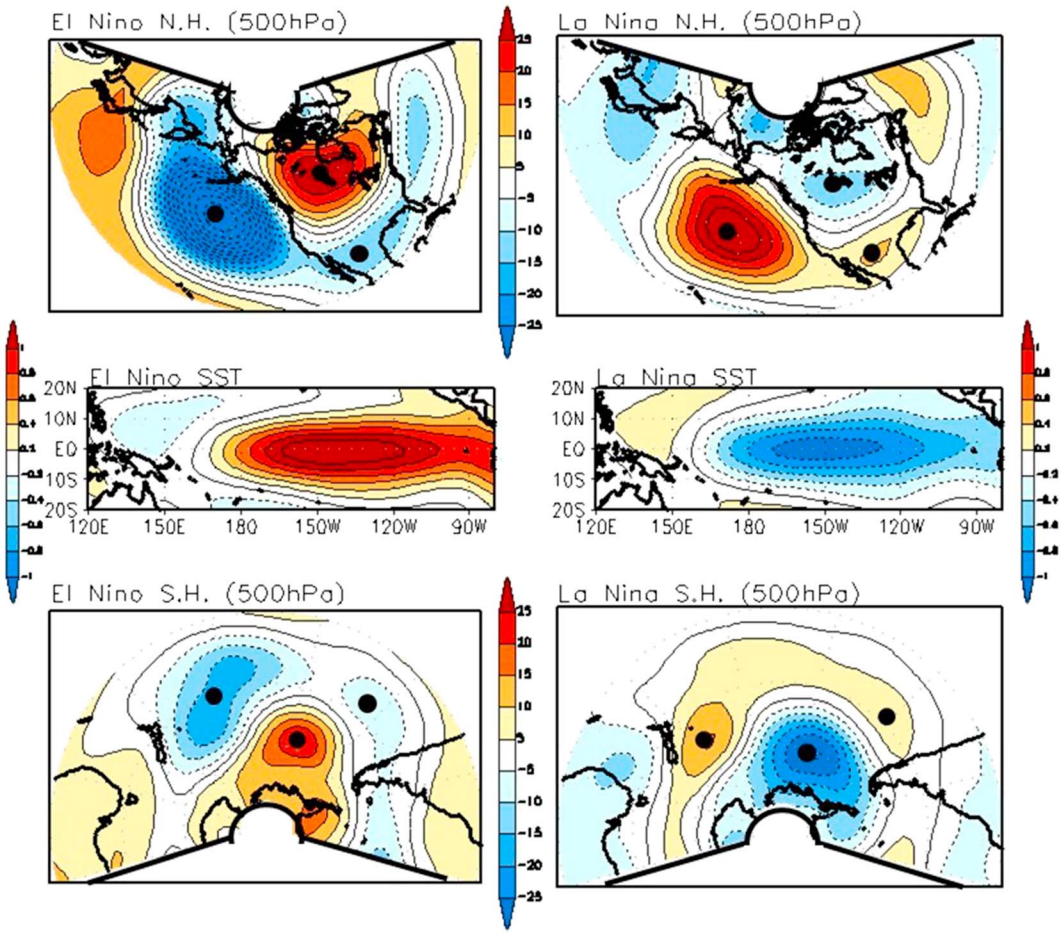

Figure 2. Composite of geopotential height (meter) at 500 hPa in boreal winter (DJF) for years of El Niños (upper left) and La Niñas (upper right). Note that the analyzed region is limited to 20°N–80°N and 120°E–330°E. Middle panels are the same as in the upper panels except for SST (°C) composite in the tropical Pacific. Lower panels are the same as in the upper panels except for the geopotential height (meter) at 500 hPa in the Southern Hemisphere. The El Niño (1982/1983, 1986/1997, 1987/1988, 1991/1992, 1994/1995, 1997/1998, 2002/2003, 2004/2005, 2006/2007, 2009/2010, 2014/2015, 2015/2016) and La Niña (1983/1984, 1984/1985, 1985/1986, 1988/1989, 1995/1996, 1996/1997, 1998/1999, 1999/2000, 2000/2001, 2005/2006, 2007/2008, 2008/2009, 2010/2011, 2011/2012) refer to the years when the NIÑO3.4 SST index during winter is greater than 0.5°C and less than −0.5°C in amplitude, respectively. The DJF NIÑO3.4 SST index is defined by time series of DJF mean SST anomaly averaged over the NIÑO3.4 region (170°W–120°W, 5°N–5°S). The seasonal mean anomaly is defined as seasonal mean deviations from a climatological (1979–2015) seasonal mean and a liner trend is removed. The SST data set is taken from the ERSST.v4. (Liu et al., 2014) and the geopotential height data set is obtained from National Center for Environmental Prediction/National Center for Atmospheric Research (NCEP/NCAR) reanalysis I (Kalnay et al., 1996). Dots denote centers of action in the ENSO teleconnections in the extratropics.

Nearly two decades ago, Diaz et al. (2001) reviewed the principal features of ENSO atmospheric teleconnections in terms of regional patterns of surface temperature, precipitation, and atmospheric circulation. They highlighted the connections between the decadal-to-multidecadal variability in tropical SSTs and ENSO properties along with decadal changes in the ENSO atmospheric teleconnections during the 20th century. In particular, Diaz et al. (2001) highlighted the periods before and after the mid-1970s when both climate states in the Pacific (Graham, 1994; Trenberth & Hurrell, 1994; Zhang et al., 1997) and ENSO characteristics (An & Wang, 2000; An et al., 2006; Fedorov & Philander, 2000; Wang & An, 2002) significantly changed. The shift in the background state over the tropical Pacific during the mid-1970s included increased SST in the eastern and central tropical Pacific (Graham, 1994). In addition, ENSO amplitude as well as its dominant period increased after the late 1970s compared to before the late 1970s (Fedorov & Philander, 2000; Wang & An, 2002). Since the 1990s, however, ENSO properties such as the spatial structure and amplitude of SST anomalies (SSTAs) as well as the ocean mean state have changed again (Capotondi et al., 2015; Jo et al., 2013, 2014, 2015; Kosaka & Xie, 2013; Lyon et al., 2014; McPhaden, 2012; McPhaden et al., 2011; Meehl et al., 2014, 2015; Xiang et al., 2013) (Figure 3). It has been observed that the center of both El Niño and La Niña SST anomalies has shifted to the

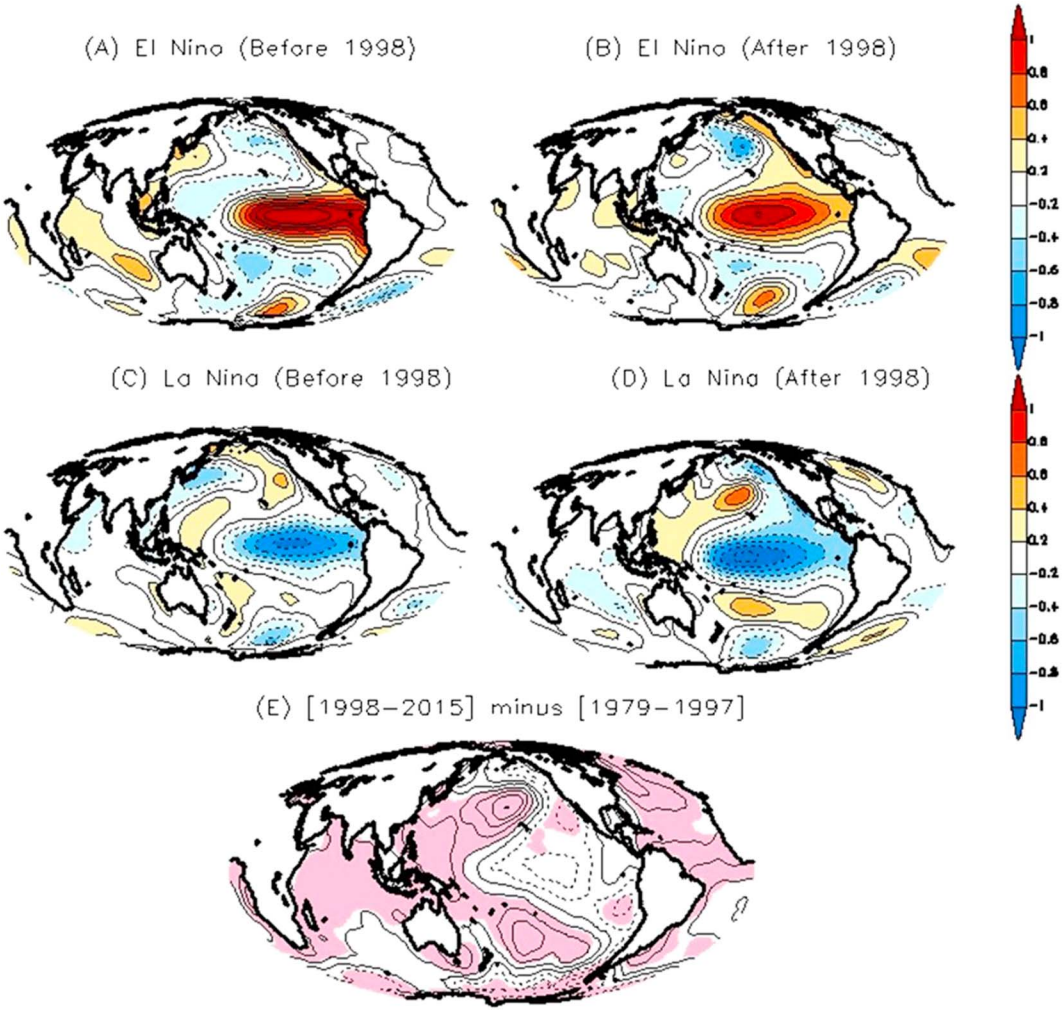

Figure 3. Composite of boreal winter SST (°C) anomalies in El Niños before (a) and after (b) late 1990s. Figures 3c and 3d are the same as in Figures 3a and 3b except for La Niña. SST anomalies are deviations from the climatological (1979–2015) mean. The mean SST difference before and after the late 1990s during boreal winter (e). Shading in Figure 3e denotes regions where the mean SST difference is statistical significant above the 95% confidence level by a *t* test. Contour interval in Figure 3e is 0.2°C. Solid and dashed line in Figure 3e denotes a positive and negative, respectively. The SST data set is taken from the ERSST.v4. (Liu et al., 2014).

west from the period of 1979–1997 compared to the period of 1998–2015 (Figures 3a–3d). Furthermore, the amplitude of El Niño events weakened from before the late 1990s to the first 15 years of the 21st century (Figures 3a and 3b). La Niña events, however, have remained relatively unchanged. On the other hand, most ocean basins have warmed since the 1990s except for the eastern Pacific, the high-latitude Southern Ocean, and the eastern North Pacific (Figure 3e). The changes of ENSO properties as well as the ocean mean state are thus different from those that occurred during the 20th century (Diaz et al., 2001).

Substantial progress in understanding ENSO dynamics, diversity, and impacts has been achieved in the past decade (Cai, Santoso, et al., 2015; Capotondi et al., 2015; Marathe et al., 2015; Yeh et al., 2014). Previous publications during this time though have provided only a brief review on impacts associated with ENSO diversity (Capotondi et al., 2015; Yeh et al., 2014) and how ENSO teleconnections associated with ENSO extremes would change under greenhouse warming (Cai, Santoso, et al., 2015). There is still a debate about the processes associated with the nonlinearity of the ENSO atmospheric teleconnections, the diversity of the ENSO atmospheric teleconnections, and the role of regional air-sea coupled processes outside the tropics in modulating the ENSO atmospheric teleconnections. These issues motivate our review of ENSO atmospheric teleconnections (hereafter, ENSO teleconnections) associated with changes in ENSO properties and ocean mean state in the tropical Pacific in recent decades and how they may change under greenhouse warming. In addition, we will show that changes in the ENSO teleconnections significantly control the

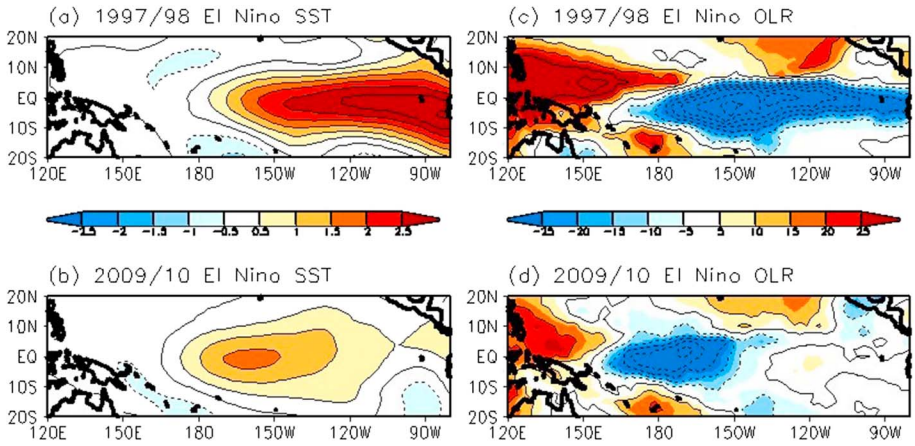

Figure 4. SST (°C) and OLR (W m^{-2}) anomalies for 1997/1998 El Niño (classified as EP El Niño, upper panel) and 2009/2010 El Niño (classified as CP El Niño, lower panel). The two types of El Niño are defined following Yeh et al. (2009). We first collect the years in which the NIÑO3 SST index during boreal winter is above 0.5°C or the boreal winter NIÑO4 SST index is above 0.5°C. Of those years, an EP-El Niño year is defined as a year in which the DJF NIÑO3 SST index is greater than the DJF NIÑO4 SST index. On the other hand, a CP-El Niño year is defined as a year in which the DJF NINO4 SST index is greater than the DJF NINO3 SST index.

statistics of extreme weather events. Finally, we will review how climate models simulate the effects of greenhouse gas forcing on ENSO teleconnections in the future.

2. ENSO's Spatial Patterns and Their Teleconnections.

Interest in ENSO teleconnections has undergone a revival in the past decade considering the diversity in ENSO spatial patterns (e.g., Capotondi et al., 2015; Trenberth & Stepaniak, 2001) (Figures 3a–3d and 4a and 4b). The recent focus has been on differences in impacts on remote temperature and precipitation between events in which the maximum anomalous SST is located in the eastern tropical Pacific (namely, Eastern Pacific El Niño) and events with maximum anomalous SST in the central tropical Pacific (namely, El Niño Modoki, Central Pacific El Niño, or Warm pool El Niño) (Ashok et al., 2007; Kao & Yu, 2009; Kug, Jin, et al., 2009) (Figures 4a and 4b). In addition, Central Pacific (CP) El Niños have occurred more frequently than Eastern Pacific (EP) El Niños since the late 1990s (Capotondi et al., 2015; Lee & McPhaden, 2010; Yeh et al., 2015), which might be due to either anthropogenic forcing (Kim & Yu, 2009; Yeh et al., 2009) or natural variability (Giese & Ray, 2011; McPhaden et al., 2011, Newman et al., 2011; Yeh et al., 2011) or both. However, there is still a debate about the robustness of these changes before and after the late 1990s because of the relatively short observational record (Stevenson et al., 2010; Wittenberg, 2009). There is also an argument that the location of El Niño SST maxima varies considerably, ranging as a continuum from the western to the eastern Pacific for the period of 1871–2008 rather than being simply bimodal with maxima in the central and eastern Pacific (Giese & Ray, 2011).

For illustrative purposes, in the following discussion we consider the existence of two extremes of the El Niño continuum associated in a statistical sense with distinct SST anomaly patterns represented by the 1997/1998 EP and the 2009/2010 CP El Niño events (Takahashi et al., 2011). ENSO teleconnections are sensitive to the longitude where atmospheric deep convection is triggered (empirically where SST $>$ 27.5 °C) (Barsugli & Sardeshmukh, 2002). These longitudes are different for EP El Niño and CP El Niño (Figures 4c and 4d), leading to different ENSO teleconnections. For example, the PNA-like Rossby waves propagating into the extratropics in the Northern Hemisphere with wave numbers of 3–4 during winter are dominant when an EP El Niño occurs (as in 1997/1998; Figure 5a). In contrast, the 500 hPa geopotential anomalies in response to CP El Niño SST forcing (as in 2009/2010) are associated with an increase in the geopotential height over the Arctic and a decrease in the surface pressure over the North Pacific and North Atlantic Ocean during winter (Figure 5b), somewhat similar to the spatial pattern of a negative phase of Arctic Oscillation (AO)-like circulation (Thompson & Wallace, 1998). In other words, the center of action for ENSO teleconnections during EP El Niño events is shifted to the east over the Eurasian continent, North America, and the North Atlantic. Conversely, during CP El Niño events, a westward shift is observed in the North Pacific. Further analysis indicates that the ENSO teleconnections during EP El Niño events and CP El Niño events are different in the Northern Hemisphere from the developing phase to the decaying phase (not shown). In particular, the

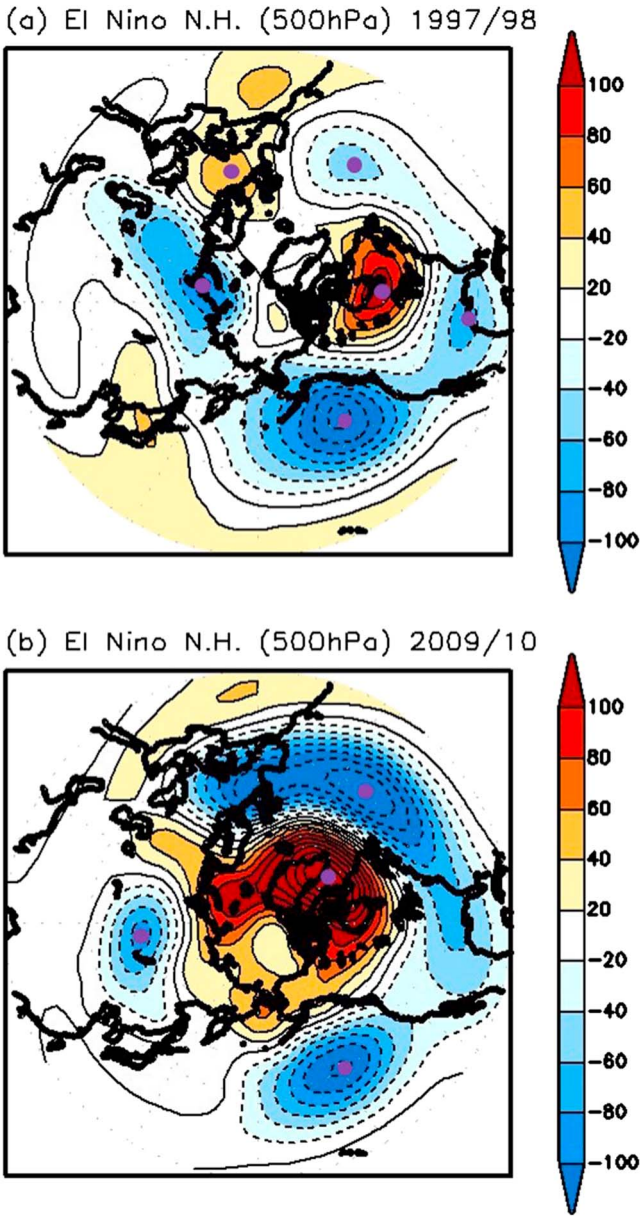

Figure 5. Figures 5a and 5b are the same as in Figures 4a and 4b except 500 hPa geopotential height (meter) anomalies during boreal winter. Dots denote centers of action in the ENSO teleconnections in the extratropics (units in meters).

location of their seasonal centers of action is shifted in the zonal and meridional direction in the high latitudes including the Arctic.

ENSO teleconnections in response to EP El Niño and CP El Niño result in different remote impacts in precipitation or temperature or both around the globe (Cai & van Rensch, 2012; Garfinkel et al., 2013; Graf & Zanchettin, 2012; Kumar et al., 2006; Mo, 2010; Preethi et al., 2015; Rodrigues et al., 2011; Taschetto & England, 2009; Wang & Hendon, 2007; Weng et al., 2007; Yu & Zou, 2013). Consequently, this diversity affects the predictability of ENSO teleconnections as well as the characteristics of extreme weather events in response to ENSO as illustrated in global land surface air temperature anomalies (Figure 6) and precipitation anomalies (Figure 7) during the 1997/1998 EP El Niño and the 2009/2010 CP El Niño winters. The spatial pattern of global surface air temperature and precipitation anomalies in response to the EP El Niño was quite different from that in response to the CP El Niño. For example, a dipole-like structure of surface air temperature anomalies over eastern North America is a dominant feature for CP El Niño, which is not the case for EP El Niño (Figures 6a and 6b). In addition, during the EP El Niño, central and eastern Europe exhibited positive surface air temperature anomalies during boreal winter, while the CP El Niño was associated with an anomalously cold winter in eastern Europe (Ashok et al., 2007; Graf & Zanchettin, 2012). It is also evident that surface air temperature anomalies in Antarctica were mirror images of one another for the EP and CP El Niños (Figures 6a and 6b). Likewise, precipitation anomalies in Europe and in Antarctic were mirror images of one another for the EP and CP El Niños (Figures 7a and 7b). Furthermore, it is found that CP El Niños are more effective in reducing the precipitation anomalies over India during the winter peak than EP El Niños, which is in contrast to eastern Australia and Mexico where the CP El Niño causes much precipitation than EP El Niño (Figures 7a and 7b).

A number of studies since the mid-2000s have focused on EP and CP El Niño teleconnections. Some studies compared differences in precipitation and temperature anomalies in response to a single EP El Niño and CP El Niño event (e.g., Figures 4–6) (Ashok et al., 2009; Barnard et al., 2011; Kumar et al., 2006; McPhaden, 2004). Others studies analyzed observed differences in teleconnection composites based on a number of EP El Niño and CP El Niño events (Ashok et al., 2007; Garfinkel et al., 2013; Graf & Zanchettin, 2012; Taschetto & England, 2009; Weng et al., 2007; Yeh et al., 2009; Yu & Zou, 2013). The interpretation of these results requires caution because of the limited number of El Niño events in the record. Thus, there are uncertainties in the precise nature of many regional ENSO precipitation and temperature teleconnections. Nevertheless, the leading ENSO teleconnection features during EP El Niño and CP El Niño, derived from available observations, provide clues on how and why EP El Niño and CP El Niño influence remote areas differently. The following summarizes the precipitation and temperature response to EP and CP El Niños for each continent based on the published literature. It should be noted, however, that these responses represent the El Niño signal against a background of considerable atmospheric noise. Correlations are relatively low suggesting that El Niño teleconnections account for only a fraction of the total variance in many parts of the globe.

2.1. The Americas

Central and northern North America experience a cooler-than-normal boreal summer before the winter peak of CP El Niño years (Weng et al., 2007). Western North America from Alaska to California is warmer in boreal summer before the winter peak of CP El Niños, but cooler or near normal during EP El Niños (Weng et al., 2007). Because of differences in teleconnections induced by EP Niño and CP El Niños, higher precipitation

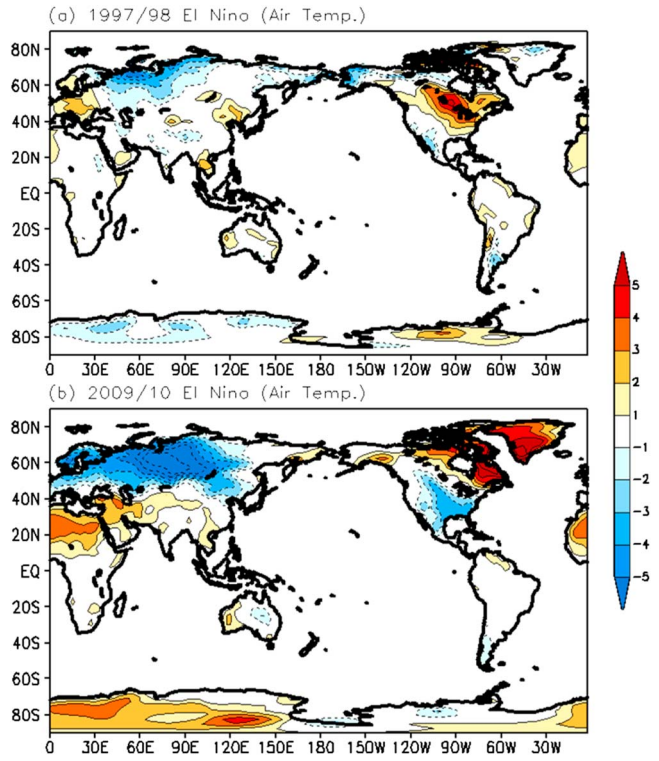

Figure 6. Figures 6a and 6b are the same as in Figures 5a and 5b except the air temperature anomalies during boreal winter. Unit in Figures 6a and 6b is °C. Note that zero contours are omitted in Figures 6a and 6b.

is observed over the Northwestern United States in boreal summer before the winter peak of EP El Niños, while higher precipitation is observed in the southwestern United States during CP El Niños (Garfinkel et al., 2013; Mo, 2010; Yu & Zou, 2013). During CP El Niños, Argentina and southern Brazil experience a warmer-than-normal austral winter, in contrast to a cooler austral winter over northern Brazil, Columbia, and Venezuela, and parts of Mexico (Ashok et al., 2007). Precipitation is below average over the Brazilian northeast in boreal spring after the winter peak of EP El Niños, in contrast to CP El Niños when the precipitation is above the average (Rodrigues et al., 2011). During EP El Niño boreal winters, the upper-level cyclonic flow taking a subtropical path over North America and Gulf Stream cyclogenesis predominantly occurs in the region where the jet streams flow to enter (Schemm et al., 2016). In contrast, during CP El Niño boreal winters, the cyclonic flow taking a northern path across North America and Gulf Stream cyclogenesis tends to occur in the region where the jet streams flow to exit. This results in the storm track differences between EP and CP El Ninos winter over the North Atlantic Ocean (Schemm et al., 2016).

2.2. Asia

A wide region in West Asia covering countries such as Turkmenistan, Kazakhstan, Armenia, and Georgia experiences cooler-than-normal conditions in boreal summer before the winter peak of CP El Niños (Ashok et al., 2007). Anomalous warm condition in boreal summer before the winter peak of CP Niños occurs in a large region from east of the Ural Mountains to the northwestern tip of northeastern China, in contrast to the almost opposite conditions that occur during EP El Niños (Weng et al., 2007). Precipitation is increased over East China and decreased over the Philippines in boreal wintertime during EP El Niños, whereas CP El Niños have a weaker effect on East China precipitation (Garfinkel et al., 2013). In recent decades, CP El Niños are more effective in reducing the Indian Monsoon rainfall in boreal summer before the winter peak and early fall than EP El Niños (Kumar et al., 2006) and thus causes severe drought over India. However, EP El Niño events that occurred in the past also have led to severe monsoon droughts over India (Rasmusson & Carpenter, 1983).

2.3. Africa

Many of the regions along the east coast of Africa experience anomalously cool conditions in boreal summer before the winter peak of CP El Niños (Ashok et al., 2007). On the other hand, during the late boreal fall and the early winter, EP El Niños are associated with an anomalous enhancement of rainfall in Eastern Africa, while CP El Niños are associated with an opposite impact (Preethi et al., 2015). Composites of temperature anomalies in boreal summer before the winter peak of CP El Niños shows warmer conditions than normal in South Africa, which was not the case in EP El Niños (Weng et al., 2007).

2.4. Australia

Australia rainfall is sensitive to the zonal distribution of SST anomalies in the tropical Pacific during ENSO events. In particular, the location of anomalously low rainfall appears to be sensitive to the zonal position of maximum SST anomalies in the equatorial Pacific (Cai & Cowan, 2009; Nicholls, 1989; Power et al., 1999; Suppiah, 2004; Taschetto & England, 2009; Wang & Hendon, 2007). A clear seasonal difference is apparent, with the maximum rainfall response for CP La Nina events occurring in austral autumn (Cai & Cowan, 2009) compared to austral spring for EP El Niño events (Taschetto & England, 2009). Rainfall across Australia during austral spring decreases more strongly during CP El Niños than during EP El Niños (Taschetto & England, 2009; Wang & Hendon, 2007). While EP El Niños are associated with a significant reduction in rainfall over northeastern and southeastern Australia during austral autumn, CP El Niños appear to drive a large-scale decrease in rainfall over northwestern and northern Australia (Taschetto & England, 2009). These ENSO teleconnections are strongly influenced by the PDO, generally weaker during a positive PDO phase.

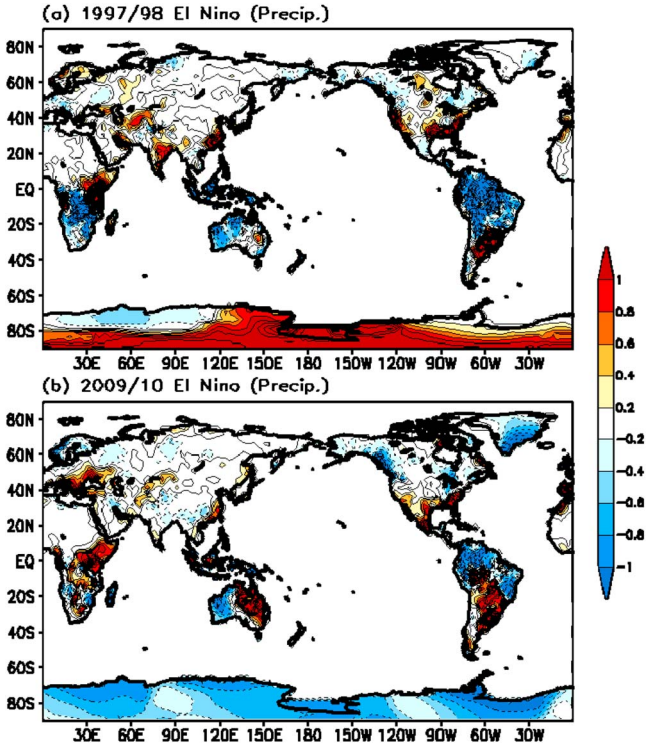

Figure 7. Figures 7a and 7b are the same as in Figures 6a and 6b except precipitation anomalies. Unit in Figures 7a and 7b is mm d^{-1}. Note that zero contours are omitted in Figures 7a and 7b.

2.5. Europe

The remote influence of EP and CP El Niños on the European sector has pathways through the North Atlantic (Brönnimann, 2007; Graf & Zanchettin, 2012; Ineson & Scaife 2009) or Arctic (Baggett & Lee, 2015; Ding et al., 2014) regions. The pathways from the tropical Pacific to the North Atlantic include a "stratospheric bridge" (Butler et al., 2014; Ineson & Scaife 2009) during EP El Niños and a "subtropical bridge" (Graf & Zanchettin, 2012) during CP El Niños. During EP El Niños, for example, central and eastern Europe experience positive surface air temperature anomalies during boreal winter; however, CP El Niño events appear to cause anomalously cold winters in eastern Europe (Ashok et al., 2007; Graf & Zanchettin, 2012). In addition, atmospheric cyclones over Gulf stream behave differently during EP El Niño and CP El Niño events, which affect the entire North Atlantic storm track, involving a more northeastward extension during CP El Niño winters than EP El Niño winters (Schemm et al., 2016). This makes CP El Niños special in their ability to produce robust European impacts during boreal winter compared to EP El Niños.

2.6. Antarctica

ENSO has been strongly linked to changes in sea ice concentration around west Antarctica (Kwok et al., 2016; Pope et al., 2017). During El Niño, a Rossby wave train emanating from the tropical Pacific is associated with a weakening of the Amundsen Sea low (Turner, 2004). This results in the so-called Antarctic dipole pattern (Kwok et al., 2016) with increased sea ice in the Bellingshausen Sea and decreased sea ice in the Ross Sea. However, there are differences in the persistence of sea ice concentration depending on whether the El Niño is an EP or CP type (Song et al., 2011; Wilson et al., 2014). During EP-El Niño events, for example, the anomalous high in the Bellingshausen Sea is replaced by an anomalous low after the austral autumn following the mature phase of the event, whereas the anomalous high pressure persists until austral winter in the case of a CP-El Niño. As a result, the Antarctic dipole in sea ice persists until austral winter after the mature phase of El Niño for a CP event but not for an EP event.

3. ENSO Teleconnections Impacted by Ocean Basins Outside the Tropical Pacific.

There is a clear influence of ENSO on SSTAs outside the tropical Pacific Ocean (Deser et al., 2010). However, the slowly evolving state of the ocean outside the tropical Pacific is able to influence not only ENSO dynamics, variability, and diversity (Dommenget & Yu, 2017), but also ENSO teleconnections through local air-sea interactions particularly in the North Pacific, the North Atlantic, and the Indian Ocean. Thus, ocean state changes outside the tropical Pacific can lead to decadal modulation of ENSO teleconnections. The mean state of most ocean basins has warmed after the late 1990s except the eastern Pacific, the high-latitude Southern Ocean and the eastern North Pacific (Figure 3e). These mean state changes are the result of natural variability, anthropogenic forcing, or their combined influence. Because there are few studies examining the influence of SSTAs outside the tropical Pacific on the teleconnections resulting from EP El Niño and CP El Niño events, the following subsection mainly describes how these remote oceans impact ENSO teleconnections without making a distinction between EP El Niño and CP El Niños.

3.1. North Pacific Ocean.

There is a slow decadal evolution of SSTAs in the Pacific referred to as Pacific Decadal Oscillation (PDO) (Mantua et al., 1997) or the Interdecadal Pacific Oscillation (IPO) (Power et al., 1999). The PDO is defined as the leading empirical orthogonal function (EOF) mode of SST in the North Pacific north of 20°N, and it is the most dominant mode of SST variability in the North Pacific on decadal timescales (Newman et al., 2016). A positive PDO is characterized by cool temperatures in the western and central North Pacific and by anomalously warm temperatures to the east, north, and south of these cool temperatures. Opposite

conditions occur during the negative phase of PDO. The PDO results from a combination of different physical processes, including local North Pacific atmosphere-ocean interactions involving reemergence of SST anomalies (Alexander et al., 1999), ENSO-forced variability from the tropics, and oceanic zonal advection of SST anomalies in the Kuroshio-Oyashio Extension. These processes operate on different timescales to collectively generate PDO-like SST anomaly patterns (Newman et al., 2016, Schneider & Cornuelle, 2005). The IPO is an alternative definition of the PDO but with an equatorial focus. As such it features a decadal timescale "ENSO-like" SST fluctuation in the Pacific, though less equatorially confined and relatively more prominent in the extratropics, especially the North Pacific, compared to ENSO (Han et al., 2014; Meehl & Hu, 2006; Power et al., 1999). A positive phase of IPO is characterized by a warm tropical Pacific and a cool extratropical Pacific and vice versa for a negative phase of IPO.

The slow evolution of SSTAs in the Pacific associated with the PDO/IPO can modulate ENSO teleconnections by interacting with the atmospheric circulation anomalies in the midlatitudes, or by changing the location of atmospheric deep convection in the tropical Pacific (Gershunov & Barnett, 1998; Hong et al., 2014). This modulation process can weaken or reinforce ENSO teleconnections on decadal timescales (Gershunov & Barnett, 1998; Hu & Huang, 2009; Kim et al., 2014; Yu & Zou, 2013). For example, during the positive phase of the PDO, or equivalently the IPO (Han et al., 2014), climate anomalies during boreal winter over North America and East Asia associated with El Niño tend to be strong and more spatially coherent (Fuentes-Franco et al., 2016; Hu & Huang, 2009; Kim et al., 2014; Kumar et al., 2016; Pavia et al., 2006). When the IPO is in a negative phase, on the other hand, the impact of La Niña on Australian precipitation is enhanced (Power et al., 1999). La Niña during a negative phase of the IPO modifies the location of the South Pacific Convergence Zone (SPCZ), which is responsible for delivering more rain-bearing cloud bands across eastern Australia (Folland et al., 2002). Usually, ENSO teleconnections around the Pacific basin are intensified when the ENSO and the PDO/IPO are in phase, and weaker when ENSO and the PDO/IPO are out-of-phase.

The phase of the PDO/IPO changed from positive to negative in the late 1990s associated with a recent decade long "hiatus" in observed globally averaged surface temperature. This period showed little increase or even a slightly negative trend of global mean surface temperature during the early 2000s (Hong et al., 2014; Kosaka & Xie, 2013; Meehl et al., 2011) though there is controversy about this issue depending on different definitions of "hiatus" and different data sets used (Medhaug et al., 2017; Risbey & Lewandowsky, 2017). This phase shift was characterized by a cooling in the eastern tropical Pacific (see Figure 3e) and a shift of the atmospheric convection to the west in the tropical Pacific during ENSO events (Jo et al., 2015; Kim et al., 2014; Xiang et al., 2013) (Figure 8). These changes result in changes in ENSO teleconnections to midlatitudes (see Figure 5). Figures 8a and 8b display the composite of anomalous outgoing longwave radiation (OLR) when El Niño occurred before and after the late 1990s, respectively. The center of negative OLR anomalies after the late 1990s is shifted to the west by about 15–20 in longitude compared to that before the late 1990s. The zonal distribution of OLR anomalies, averaged between 2.5°N and 2.5°S, before and after the late 1990s supports this notion (Figure 8c). Similarly, for La Niña, the center of positive OLR anomalies also shifted to the west by about 10° longitude from the late 1990s to after the late 1990s (Figures 8d–8f). It is known that the OLR is a proxy for atmospheric heating, anomalies of which force changes in atmospheric circulation that affect the middle-to-high latitudes (Chiodi & Harrison, 2015). These changes in OLR lead to altered forcing of the large-scale atmospheric Rossby waves by changing convergence patterns in the lower and upper atmosphere (Hoskins & Karoly, 1981), modulating the atmospheric teleconnections into the middle-to-high latitudes. For example, the anomalous Aleutian low pressure associated with El Niño events became deeper and its center shifted southwestward after the late 1990s primarily due to the westward shift in the location of the tropical convective heating around the dateline (see Figures 8a and 8b) that occurred after the late 1990s (Jo et al., 2015).

3.2. Atlantic Ocean

It is well documented that following the peak development of El Niño during boreal winter the tropical North Atlantic Ocean becomes anomalously warm during the subsequent boreal spring and early summer (Huang, 2004; Klein et al., 1999; Trenberth et al., 2014); similarly, the tropical North Atlantic Ocean tends to cool following the peak of La Niña events. The strength of the connection between El Niño and tropical north Atlantic SST anomalies depends on whether it is an EP El Niño or a CP El Niño (Taschetto et al., 2016). There is also evidence that positive Atlantic SST anomalies north of the equator (0–20°N) plays a significant role in

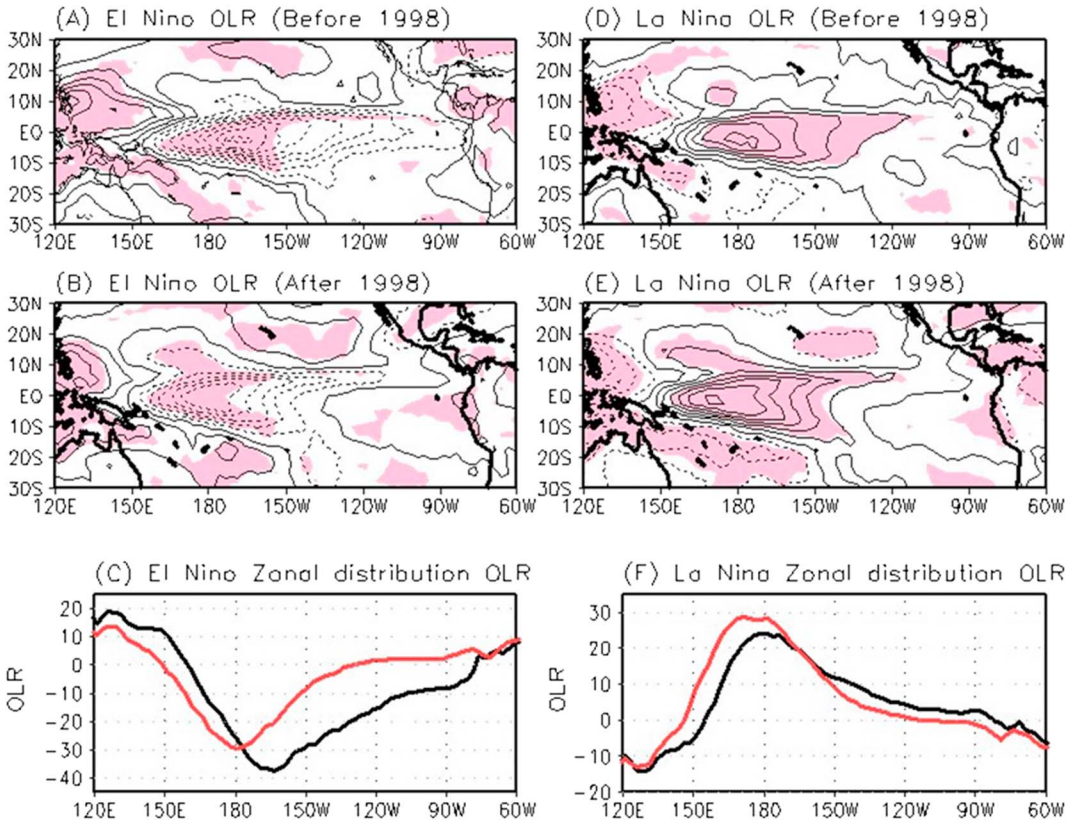

Figure 8. Composite of boreal winter OLR (W m^{-2}) anomalies in El Niños before (a) and after (b) late 1990s. Figures 8d and 8e are the same as in Figures 8a and 8b except for La Niña. OLR anomalies are deviations from the climatological (1979–2015) mean. Contour interval in Figures 8a, 8b, 8d, and 8e is 5 W m^{-2}. The *y* axis in Figure 8c is the zonal distribution of OLR (W m^{-2}) anomalies averaged in 2.5°N–2.5°S of El Niños before (black) and after (red) late 1990s. Figures 8f is the same as in Figure 8c except for La Niña Nina. Unit in Figures 8c and 8f is W m^{-2}. Shading in Figure 8 denotes regions where the composited OLR anomalies are statistical significant above the 95% confidence level by *t* test.

modulating ENSO teleconnections and their impact on the North Atlantic and Europe (Ham et al., 2014; Kumar & Hoerling, 2003). An off-equatorial (0–20°N) North Atlantic SST anomaly intensifies the North Atlantic Oscillation-like atmospheric variability through local air-sea coupled processes (Sung et al., 2013), which, in turn, modulates ENSO teleconnections over the North Atlantic and Europe. Note that such positive Atlantic SST anomalies north of the equator are distinct from the positive or warm phase of the Atlantic Multidecadal Oscillation (AMO) (Enfield et al., 2001), which is defined as basin-wide (0–60°N) warming of the North Atlantic on multidecadal timescales. In the presence of an Atlantic SST warming north of the equator, El Niño teleconnections exhibit a north-south dipole-like structure in geopotential height over the Atlantic/Western Europe sector as well as a deepening of the Aleutian low over the North Pacific sector (Ham et al., 2014).

There is also an interhemispheric SST gradient mode in the Atlantic Ocean (Okumura et al., 2001), which is more tropically confined than the AMO and can interfere with ENSO teleconnections in the Atlantic (Giannini et al., 2000, 2001, Rodrigues & McPhaden, 2014). The dipole-like SST anomaly across the equator forces atmospheric anomalies through a positive wind-evaporation-SST feedback (Xie & Philander, 1994), the influence of which can extend to the extratropics (Handoh et al., 2006) to obscure or reinforce ENSO atmospheric teleconnections. These results suggest that the state of the Atlantic Ocean SST may play a role in modulating ENSO teleconnections in the Atlantic and European region.

3.3. Indian Ocean

The Indian Ocean is home to some of the warmest water in the world's ocean, exceeding 28°C (Tao et al., 2015). Therefore, deep convection is active over this warm water and is a key source for atmospheric teleconnections into both hemispheres (Xie et al., 2016). The atmospheric teleconnection patterns due to the two

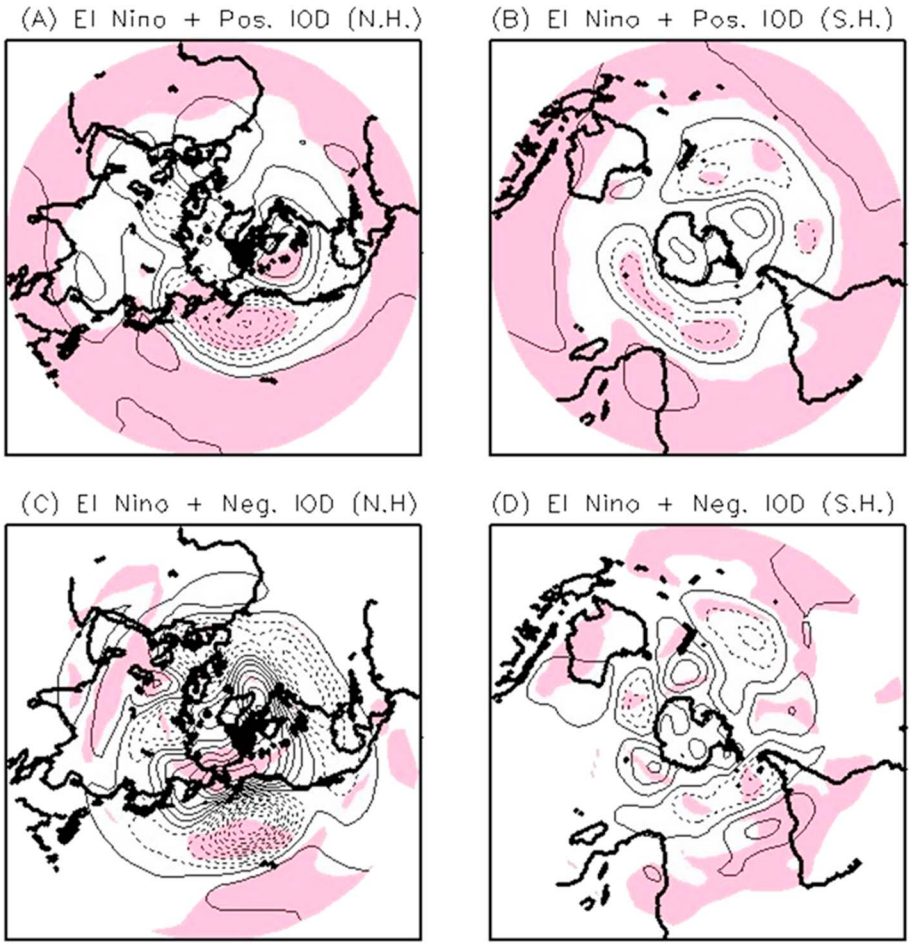

Figure 9. Composite of geopotential anomalies (meter) in El Niños during boreal winter accompanied by a positive IOD in the previous fall in the Northern Hemisphere (a) and the Southern Hemisphere (b). Figures 9c and 9d are the same as in Figures 9a and 9b except El Niños during boreal winter accompanying with a negative IOD in the previous fall. See the composite years in Table 1. Solid line denotes are positive, and dashed line denotes negative. Contour interval is 10 m and shading in Figure 9 denotes regions where the composited geopotential anomalies are statistically significant above the 95% confidence level according to a *t* test.

major modes of Indian Ocean SST variability, the Indian Ocean Basin Mode (IOBM), and Indian Ocean Dipole (IOD) (Saji et al., 1999) have different geographical locations in terms of their center of actions compared to ENSO teleconnenctions (Cai et al., 2011). The IOBM can be defined as the first EOF of Indian Ocean SST anomalies, and the IOD is defined as the difference of the area mean SST anomalies in the western Indian Ocean (10°S–10°N, 50–70°E) and the eastern Indian Ocean (10°S–0°, 90–110°E) (Saji et al., 1999). While a positive (negative) phase of IOBM is characterized by a basin-wide warming (cooling) in the Indian Ocean, a positive (negative) phase of the IOD indicates an anomalous warm (cold) SST in the western Indian Ocean and an anomalous cold (warm) SST in the eastern Indian Ocean with a dipole-like structure in the zonal direction. The driving mechanisms for the IOBM and the IOD are different (Saji et al., 1999, Webster et al., 1999), though both exhibit a strong seasonality. That is, the peak intensity of the IOBM is observed in boreal winter, while the IOD peaks in boreal fall (An, 2004), leading a phase shift between IOBM and IOD (An, 2004; Ha et al., 2016).

ENSO impacts are modulated by the IOD in the Northern and Southern extratropics during boreal winter (Saji & Yamagata, 2003; Tao et al., 2015). For example, wave trains like the PNA and the PSA are prominent during El Niño in the boreal winter when accompanied by a positive IOD in the previous fall (Figures 9a and 9b). In contrast, atmospheric teleconnections across the Arctic and the Antarctic are observed in the Northern and Southern Hemispheres, respectively, in the case of El Niño accompanied by a negative IOD in the previous boreal fall (Figures 9c and 9d). However, the regions where a high level of statistical significance of

Table 1
The Year of El Niño and La Niña Events During Boreal Winter Accompanying With a Positive and Negative IOD in Previous Fall (September-October-November), Respectively

	El Niño during boreal winter	La Niña during boreal winter
Positive IOD in previous fall	1982/1983, 1986/1987, 1987/1988, 1991/1992, 1994/1995, 1997/1998, 2002/2003, 2004/2005, 2006/2007, 2015/2016	1983/1984, 1985/1986, 2007/2008, 2008/2009, 2011/2012
Negative IOD in previous fall	2009/2010, 2014/2015	1984/1985, 1988/1989, 1995/1996, 1996/1997, 1998/1999, 1999/2000, 2000/2001, 2005/2006, 2010/2011

Note. El Niño (La Niña) refer to the years when the NIÑO3.4 SST index during boreal winter (December-January-February, DJF) is greater (less than) than 0.5°C (−0.5°C) in amplitude. The DJF NIÑO3.4 SST index is defined by time series of DJF mean SST anomaly averaged over the NIÑO3.4 region (170°W–120°W, 5°N–5°S). The IOD index is defined as the difference in SST anomaly between the tropical western Indian Ocean (50°E–70°E, 10°S–10°N) and the tropical southeastern Indian Ocean (90°E–110°E, 10°S to equator) during boreal fall (Saji et al., 1999). The seasonal mean anomaly is defined as seasonal mean deviations from a climatological (1979–2015) seasonal mean and a liner trend is removed. The SST data set is taken from the ERSST.v4. (Liu et al., 2014).

atmospheric teleconnections are reached are very limited in the midlatitudes of both hemispheres (Figures 9c and 9d).

In addition, a positive IOD is associated with development of the East Indian Ocean wave train, resulting in an equivalent barotropic ridge over southern Australia, leading to less rainfall than usual over much of southern Australia during austral winter (Cai et al., 2011). Furthermore, the number of times El Niño occurs with a positive IOD is larger than the number of times when El Niño occurs with a negative IOD. In contrast, the number of frequency of La Niñas occurring with a negative IOD is larger than for La Niñas with a positive IOD (Table 1). There are clear asymmetries in the spatial pattern of rainfall in the tropical Pacific between an El Niño concurrent with a positive IOD (Figure 10a), and a La Niña concurrent with a negative IOD (Figure 10b) (Cai et al., 2011, 2012; Tao et al., 2015), resulting in an asymmetry in impact, including greater precipitation anomalies in the central tropical Pacific in El Niño events concurrent with a positive IOD (Figure 10c).

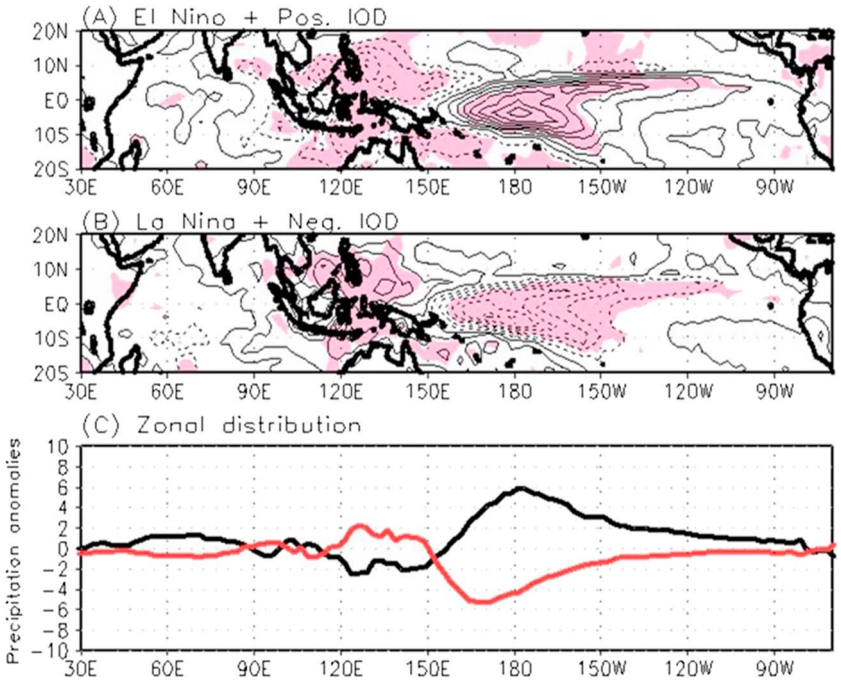

Figure 10. Composite of precipitation anomalies (mm d^{-1}) in El Niños during boreal winter accompanied by with a positive IOD in the previous fall (a) and the La Niñas during boreal winter accompanied by a negative IOD in the previous fall (b). Solid line denotes are positive and dashed line denotes negative. Contour interval is 1 mm d^{-1} and shading in Figures 10a and 10b denotes regions where the composited precipitation anomalies are statistically significant above the 95% confidence level according to a *t* test. The *y* axis in Figure 10c is the zonal distribution of precipitation anomalies averaged in 2.5°N–2.5°S of El Niños with a positive IOD (black) and La Niña with a negative IOD (red). Unit is mm d^{-1}. The winter mean anomaly is defined as winter mean deviations from a climatological (1979–2015) winter mean with a liner trend removed. The precipitation data set is taken from CPC Merged Analysis of Precipitation (CMAP) version is from https://www.esrl.noaa.gov/psd/data/gridded/data.cmap.html.

The South Asian High, which forms near the tropopause over the Indochinese peninsula before the Bay of Bengal monsoon onset in the late spring, is stronger than normal when El Niño occurs, leading to less precipitation in the following summer over East Asia (Wei et al., 2014). However, South Asian High is stronger when a positive IOBM in previous winter is concurrent with El Niño, while not as clear when not accompanied by an IOBM (Yang et al., 2007). Following an El Niño event in the previous winter, for example, a positive IOBM persists through boreal summer and leads to an increase of precipitation in the Indian Ocean. This leads to stronger than usual South Asian High through a Matsuno-Gill-type response (Gill, 1980; Matsuno, 1966), which is characterized by the quasi-steady response via the equatorial Rossby and Kelvin waves to a given tropical atmospheric heating in the Indian Ocean (Yang et al., 2007). Subsequently, this causes less precipitation over East Asia in summer as suggested in Sun et al. (2011). Similarly, ENSO characteristics including evolution, spatial pattern, and amplitude can be altered by interbasin interactions involving the IOBM, the IOD, and ENSO (Ha et al., 2016; Okumura et al., 2011), which modifies ENSO teleconnections. The pathway of ENSO teleconnections from the tropical western Pacific to East Asia can be altered by the state of IOBM, with a positive phase exciting a low-level anticyclonic circulation over the subtropical Northwest Pacific. This leads to changes in the centers of action in the Pacific-Japan-like atmospheric teleconnections forced by convective forcing related to ENSO, affecting precipitation variability in East Asia during summer by changing the transport of moisture (Ding et al., 2011).

4. Extreme Events Due To ENSO Teleconnections

This section reviews studies of the influences of ENSO on extreme events without consideration of whether events are of the EP or CP type, since there are few studies comparing the differing influences of EP and CP El Niños on these events. This limitation is mainly due to the limited availability of long-term daily observations over the globe, particularly precipitation data over ocean areas.

ENSO can affect the intensity and occurrence of extreme events such as heat waves, droughts, and floods (King et al., 2016). Using available indices to represent frequency and intensity of extremes, a few of studies have investigated global response patterns of extremes to ENSO over land areas where reasonably long observational records exist (Kenyon & Hegerl, 2008, 2010; Meehl, Tebaldi, et al., 2007). These studies find that temperature and precipitation extremes over many land areas are affected by ENSO teleconnections, showing statistically significant (5%) differences between El Niño and La Niña years and that the response patterns for extremes to ENSO basically follow the mean ENSO teleconnection patterns.

ENSO's influence on temperature extremes occurs globally, but most profoundly around the Pacific Rim and over North America (Arblaster & Alexander, 2012; Kenyon & Hegerl, 2008). Extreme maximum temperatures increase markedly during El Niño over India, Southeast Asia, Australia, and southern Africa while temperatures become cooler over southeastern North America, and vice versa during La Niña. Precipitation extremes, throughout the world, are also affected by ENSO although responses are less spatially coherent than those for temperature extremes (Kenyon & Hegerl, 2010). During boreal winter, El Niño induces statistically significant (5%) increases in precipitation extremes over southwestern North America, Central America, South America and India, while Australia, southern Africa, Southeast Asia, and Canada experience reductions in heavy precipitation (Figures 11a–11d). Extreme rainfall in northern Peru and Ecuador were particularly notable during the extreme El Niño events such as 1982/1983 and 1997/1998 (Pineda et al., 2013). La Niña brings generally opposite responses, and these response patterns of precipitation extremes generally follow the total precipitation responses.

Coupled climate models, which exhibit a wide range of behaviors in the simulation of ENSO events and thus varying teleconnection patterns (Meehl, Stocker, et al., 2007; Langenbrunner & Neelin, 2013), also indicate a close relationship between the responses of seasonal means and seasonal extremes. This is not unexpected, but there are no studies confirming this relationship in the observations. Figure 12 shows spatial correlation coefficients (bars) between the mean precipitation response and the extreme precipitation response to ENSO obtained from each CMIP5 model compared to that from the National Center for Environmental Prediction/National Center for Atmospheric Research (NCEP/NCAR) reanalysis. Overall, high spatial correlations exist in all the models with multimodel mean values being very similar to the observed ($r > 0.7$). The high values of correlation indicate consistent teleconnection patterns between mean climate and extremes to ENSO for a given model. Studies of regional extremes related to ENSO teleconnections find a good agreement

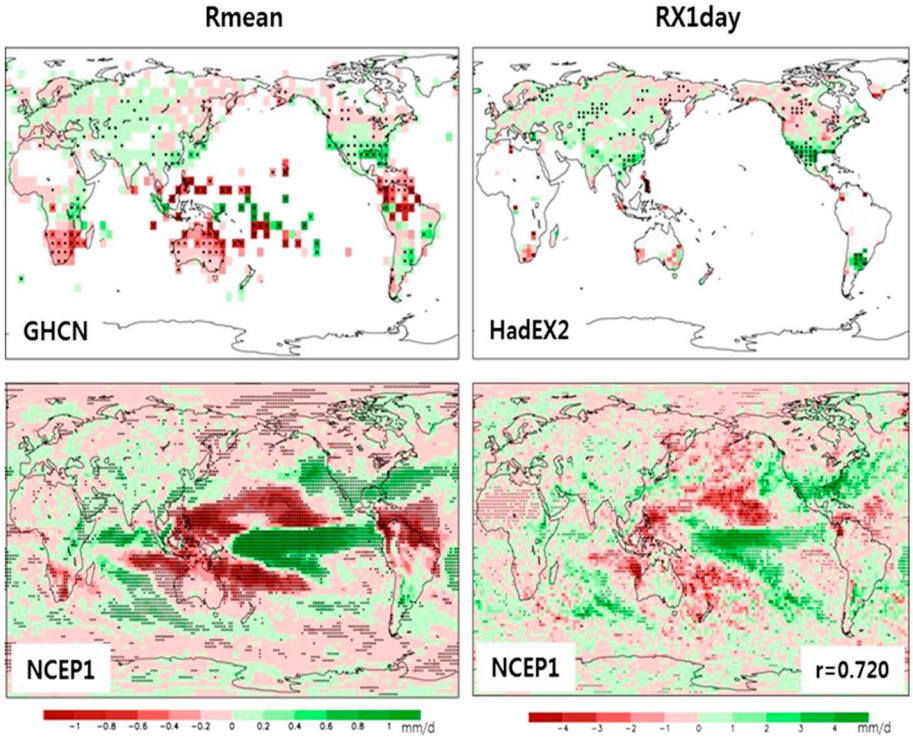

Figure 11. ENSO influence on DJF total precipitation (Rmean, left) and DJF maxima of daily precipitation (RX1day, right) during 1950/1951–2009/2010. Regression coefficients of (left) Rmean (unit: mm per standard deviation) of station-based Global Historical Climatology Network (GHCN) observations (upper) and NCEP/NCAR reanalysis data set (NCEP1, lower) onto the NIÑO3.4 index (left), and regression coefficients of Generalized Extreme Value (GEV) location parameter of RX1day (right) onto the NIÑO3.4 index using HadEX2 observations (upper) and NCEP/NCAR reanalysis (lower). NIÑO3.4 index is detrended and normalized prior to analysis. Grids with dots indicate statistical significant regressions at 5% level. In the observed analysis, only grid points having data for longer than 80% of the analysis period are included.

between the seasonal mean and seasonal extreme responses (Gershunov & Barnett, 1998). For example, drier and hotter conditions in both means and extremes occur over northeastern and southern Australia during El Niño, while wetter and cooler conditions prevail during La Niña (Min et al., 2013). This mean-extreme relationship is found for ocean wave heights over northeastern North Pacific with increases during El Niño and decreases during La Niña (Kumar et al., 2016). An opposite response occurs over the tropical western Pacific and Indian Oceans, in accord with ENSO's general impact on sea level pressure and the associated

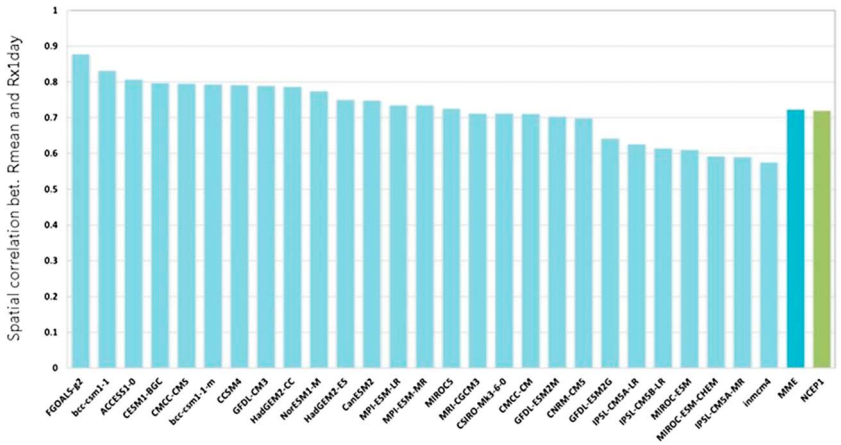

Figure 12. Spatial correlation coefficients between the global response pattern of DJF total precipitation (Rmean) and that of DJF extreme precipitation (seasonal maxima of daily precipitation, RX1day) to ENSO for each CMIP5 models (historical simulations for 1950–2005 combined with RCP4.5 scenario simulations for 2006–2010), multimodel ensemble mean of correlation coefficients (MME), and the NCEP1 reanalysis (as shown in the lower panels of Figure 11).

wind speed. This also supports the prominent impact of ENSO on coastal erosion and flooding across the Pacific (Barnard et al., 2015). Meehl, Tebaldi, et al. (2007) also showed that projections for the patterns of extremes over the U.S. during future El Niño events are expected to change because El Niño teleconnection patterns over the U.S. are projected to shift eastward and northward in a warmer climate. This mean-extreme relation in terms of ENSO teleconnections in both observations and models indicates the likelihood that the same physical mechanisms are at work. The strong physical link between seasonal mean and seasonal extreme response implies that reducing biases in mean responses may improve the simulation of extremes.

There remain large uncertainties, however, in understanding, evaluating, and predicting ENSO-induced changes in extreme events. Challenges include asymmetric nonlinear responses of extremes to El Niño and La Niña, influences of EP/CP El Niños on extremes in terms of amplitude, frequency, and duration, decadal modulation of ENSO impacts on extremes, and identification of global warming signals in extreme responses to ENSO teleconnections. With respect to nonlinear responses, impacts of extreme ENSO events on the strength and pattern of teleconnections need to be studied together with underlying physical mechanisms given that extreme El Niño/La Niña events are expected to occur more frequently after the mid 21st century. This expectation is based on coupled model simulations forced with Representative Concentration Pathways (RCP) 8.5 scenario (Cai, Wang, et al., 2015; Cai et al., 2014), where the RCP8.5 scenario denotes a greenhouse gas concentration trajectory with a radiative forcing of +8.5 W/m^2 in the year 2100 (IPCC, 2013). Overall, ENSO teleconnections influence both seasonal mean climate on interannual timescales and seasonal weather and climate extremes, with similar spatial patterns. This relationship provides important implications for evaluating the ability of models to simulate weather and climate extremes in the present climate and also for future climate projections (Arblaster & Alexander, 2012; Min et al., 2013).

5. ENSO Teleconnections Under Global Warming

Changes in ENSO teleconnections under global warning will be largely dependent on two factors, i.e., changes in the mean state both in the tropical Pacific and elsewhere around the globe and changes in ENSO properties such as its spatial pattern and amplitude. These two factors may lead to changes in both the intensity and the location of convective heating associated with ENSO, resulting in the changes in ENSO teleconnections (Cai, Santoso, et al., 2015; Dommenget & Yu, 2017). Furthermore, global warming can intensify the nonlinear tropical precipitation response to El Niño events, which may add more complexity of ENSO teleconnections in a warmer world (Power et al., 2013).

Analyses of Coupled Model Intercomparison Project Phase 3 (CMIP3) and Phase 5 (CMIP5) climate models under greenhouse warming show that models disagree considerably on future changes in ENSO properties (Cai, Santoso, et al., 2015; Collins et al., 2010; Ham & Kug, 2016; IPCC, 2013; Meehl, Stocker, et al., 2007; Zheng et al., 2016), but they generally indicate that warming of the background state on which ENSO events develop is likely to be faster in eastern tropical Pacific than in the western tropical Pacific. Because of the thermodynamic scaling of temperature and precipitation in a warmer climate (Held & Soden, 2006), the strength of the zonally asymmetric atmospheric circulation in the tropics (i.e., the Walker circulation) decreases in future climate experiments according to CMIP3 and CMIP5 climate models. This induces substantial changes to the thermal structure and circulation of the tropical oceans by decreasing the frequency of strong updrafts and increasing the frequency of weak updrafts, resulting in "El Niño-like" conditions in the tropical Pacific mean state (Vecchi & Soden, 2007).

There exists a relationship between the ENSO amplitude and the mean precipitation over the eastern tropical Pacific in CMIP5 climate models, i.e., a wetter mean state with greater precipitation acts to increase ENSO amplitude by strengthening positive coupled feedbacks in future climate (Watanabe et al., 2012). Also, tropical Pacific SST trends are projected to lead to substantial changes in the spatial patterns of ENSO-driven variability in surface temperature and precipitation of the tropical Pacific (Vecchi & Wittenberg, 2010). These changes are likely to lead to changes in ENSO teleconnections (Kug, An, et al., 2009; Meehl & Teng, 2007; Müller & Roeckner, 2008; Schneider et al., 2009; Stevenson, 2012; Zhou et al., 2014) as described next.

There is an expected eastward shift of the PNA teleconnection pattern under global warming (Kug, An, et al., 2009; Meehl, Stocker, et al., 2007; Zhou et al., 2014), resulting from a systematic eastward migration of convection centers associated with both El Niño and La Niña in the CMIP3 climate models (Müller & Roeckner, 2008; Power et al., 2013). In a warmer climate, precipitation anomalies are enhanced and they move eastward

over the equatorial Pacific because the enhanced mean SST warming in the eastern basin reduces the barrier to deep convection there. Such an eastward shift in tropical convective anomalies can cause ENSO-forced PNA teleconnections to shift eastward and to intensify under greenhouse warming (Müller & Roeckner, 2008). There is also the possibility that in a warmer climate these teleconnections may contribute to altering the basic state in the midlatitudes, leading to a change in the intensity and the position of midlatitude Rossby waves associated with ENSO convective heating anomalies (Branstator & Selten, 2009). That is, global warming can cause a two-way interaction between the trend of atmospheric basic state and the modes of variability such as PNA. On the other hand, it has been suggested that El Niño teleconnections could weaken due partly to an increase in the static stability of the atmosphere in the midlatitudes (Schneider et al., 2009). In contrast, La Niña teleconnections under global warming are likely to strengthen the Aleutian low, although with a smaller mean eastward shift in the CMIP5 climate models than in the CMIP3 climate models (Stevenson, 2012).

Recently, studies with precipitation-based ENSO indices have suggested that the frequency of extreme El Niño and La Niña events will increase after the mid-21st century under the RCP8.5 scenario (Cai et al., 2014; Cai, Wang, et al., 2015), possibly causing more severe weather and climate variations under a very high CO_2 concentrations above 650 ppm. Furthermore, it has been suggested that extreme El Niño frequency increases linearly with the global mean temperature before 2050 toward a doubling at 1.5°C warming under the RCP2.6 scenario and that an increasing frequency of extreme El Niño events continues for up to a century after global mean temperature has stabilized (Wang et al., 2017). The dominant mode of global precipitation-evaporation variability on interannual timescales is mainly due to ENSO teleconnections on interannual timescales. Therefore, the increase in frequency of extreme ENSO events may cause more severe droughts and floods in a warmer climate, with largest increases in the tropical Pacific and polar regions (Christensen et al., 2013; Seager et al., 2012). It has also been noted that as the specific humidity of the atmosphere increases with warming according to the Clausius-Clapeyron relation, the same circulation patterns as a present could produce more moisture convergence and hence more rainfall; therefore, even in the absence of any changes in ENSO properties, there would be increase in ENSO-related precipitation anomalies (Power et al., 2013; Seager et al., 2012). However, there is also a general weakening of the tropical circulation, and the associated dynamical effect could offset the thermodynamic impact due to an increase in specific humidity (Chadwick et al., 2013; Huang & Xie, 2015).

Changes in tropical Pacific mean SST and ENSO properties under greenhouse warming will thus likely continue to alter ENSO teleconnections due to changes in mean state of the atmosphere over the globe as evident in the current CMIP3 and CMIP5-type class climate models. However, future ENSO teleconnection changes do not currently show strong intermodel agreement from region to region, which is mostly due to the uncertainty of model physics and thermodynamics in accounting for the sensitivity for the climate variability to global warming. Therefore, it is important to identify which factors affect uncertainty in future model projections.

6. Summary and Discussion

ENSO properties including the spatial pattern and amplitude and the ocean mean state outside the tropics have changed over the past few decades, which might be due to anthropogenic forcing, natural variability, or their combination. This has resulted in changes in ENSO teleconnections, as manifested by changes in the centers of action of associated anomalous atmospheric circulation in the extratropics. These changes in ENSO teleconnections also lead to a different response in precipitation, temperature, or both around the globe. In addition, changes in ENSO teleconnection patterns have affected the statistics of extreme events in temperature and precipitation and the predictability of teleconnection impacts. ENSO teleconnections differ in detail from event to event. They can be also influenced by conditions outside the tropical Pacific Ocean and modified by a longer timescale climate phenomenon. Furthermore, nonlinearities in global ENSO teleconnections strongly complicate the investigation of ENSO-related climate variability. Van Oldenborgh and Burgers (2005) also propose that precipitation variability due to ENSO teleconnections could be explained by random fluctuations on decadal timescales.

ENSO teleconnections are not stationary and their predictability is not high except for certain regions such as Indonesia, eastern Australia, and eastern Africa, thus representing one of the key challenges for weather and climate prediction. For example, the 2015/2016 El Niño event was one of the strongest El Niño in recent

history, rivaling the previous two strong El Niño events in 1982/1983 and 1997/1998. However, the temperature and precipitation anomalies due to the 2015/2016 El Niño differed from the expectation associated with previous strong El Niño events (Jong et al., 2016, Nicolas et al., 2017, Kumar & Chen, 2017). For example, the very strong 1982/1983 and 1997/1998 El Niños brought heavy rains to California during the winter season, which was not the case in the 2015/2016 El Niño. On the other hand, unlike during the strong 1982/1983 and 1997/1998 El Niños, the unusual extent and duration of the melting in west Antarctica was likely favored by the strong 2015/2016 El Niño event.

It should be also noted that the statistical significance of the changes in precipitation, temperature, and extreme events due to the changes in ENSO teleconnections is marginal in many regions. There is still a debate about the robustness of the changes in ENSO properties and its teleconnections before and after the late 1990s because of the short observational record (Fedorov & Philander, 2000; McPhaden et al., 2011; Stevenson et al., 2010; Wittenberg, 2009). It has also been pointed out that it may be more appropriate to use atmospheric parameters more directly related to forcing of teleconnections such as OLR, which is a measure of deep atmospheric convection, rather than conventional SST indices to assess the far-field impacts of ENSO (Cai et al., 2014; Chiodi & Harrison, 2013, 2015). Better understanding of how large-scale environmental conditions during ENSO events determine OLR and deep atmospheric convection will lead to improved seasonal precipitation forecasts for many areas of the globe. A further complicating factor is nonlinearity in ENSO teleconnections, which result from a combination of nonlinearities in ENSO SST variability and nonlinearities in the atmospheric response to a given ENSO SST anomaly (Frauen et al., 2014).

To understand ENSO teleconnections under global warming, it is crucial to realistically simulate changes in the mean state of the tropical Pacific Ocean and the changes in ENSO properties including spatial pattern and amplitude. These factors are closely associated with the changes in the intensity and the location of tropical convective forcing, which ultimately determine the characteristics of ENSO teleconnections. In particular, the current CMIP-class climate models still suffer from the double Intertropical Convergence Zone (ITCZ) syndrome, which is characterized by a mean precipitation pattern that is too symmetric near the equator associated with an overly zonal SPCZ (Bellucci et al., 2010; Li & Xie, 2014; Lin, 2007). Such mean state bias affects ENSO mechanisms, variability, and asymmetry (Bellenger et al., 2013, Guilyardi et al., 2004, 2009, Lloyd et al., 2011) in the Pacific and also the nature of ENSO teleconnections in the midlatitudes. Simulation of the mean precipitation pattern in the ITCZ/SPCZ is tightly linked to the ability of models to correctly simulate the pattern and magnitude of mean SST in the tropical Pacific. In addition, the CMIP-class climate models have a persistent warm bias in eastern boundary current systems (Richter, 2015), which has a large influence on regional air-sea interactions and ENSO teleconnections. Therefore, improvements in model realism for these features are likely to lead to improvements in the realism of simulated ENSO teleconnection patterns and in the confidence of future regional responses to greenhouse warming.

Acknowledgments

We acknowledge the World Climate Research Programme's Working Group on Coupled Modeling, which is responsible for CMIP, and we thank the climate modeling groups for producing and making available their model outputs. The ERSST.v4 data set is from https://www.ncdc.noaa.gov/data-access/marineocean-data/extended-reconstructed-sea-surface-temperature-ersst-v4 and the CPC Merged Analysis of Precipitation (CMAP) version is from https://www.esrl.noaa.gov/psd/data/gridded/data.cmap.html. The NCEP and NCAR global reanalysis atmospheric variables can also be obtained from Earth System Research Laboratory (http://www.errl.noaa.gov/psd/data/gridded/data.ncep.reanlaysis.html). The OLR data set is obtained from https://www.esrl.noaa.gov/psd/map/clim/olr.shtml. S. W. Y. is supported by the Korea Meteorological Administration Research and Development Program under grant KMIPA2015-2112. Wenju Cai is supported by Earth System and Climate Change Hub of the Australia National Environmental Science Programme, and Centre for Southern Hemisphere Oceans Research, an international collaboration between CSIRO and Qingdao National Laboratory for Marine Sciences and Technology. B. Dewitte acknowledges supports from FONDECYT (1151185) and from LEFE-GMMC. Dietmar Dommenget is supported by ARC Centre of Excellence for Climate System Science (CE110001028). This is PMEL contribution 4735.

References

Alexander, M. A., Blade, I., Newman, M., Lanzante, J. R., Lau, N. C., & Scott, J. D. (2002). The atmospheric bridge: The influence of ENSO teleconnections on air–sea interaction over the global oceans. *Journal of Climate*, *15*, 2205–2231.

Alexander, M. A., Deser, C., & Timlin, M. S. (1999). The reemergence of SST anomalies in the North Pacific Ocean. *Journal of Climate*, *12*, 2419–2433.

An, S.-I. (2004). A dynamic link between the basin-scale and zonal modes in the tropical Indian Ocean. *Theoretical and Applied Climatology*, *78*, 203–215.

An, S.-I., & Wang, B. (2000). Interdecadal change of the structure of the ENSO mode and its impact on the ENSO frequency. *Journal of Climate*, *13*, 2044–2055.

An, S.-I., Ye, Z., & Hsieh, W. W. (2006). Change in the leading ENSO modes associated with the late 1970s climate shift: Role of surface zonal current. *Geophysical Research Letters*, *33*, L14609. https://doi.org/10.1029/2006GL026604

Arblaster, J. M., & Alexander, L. V. (2012). The impact of the El Niño-Southern Oscillation on maximum temperature extremes. *Geophysical Research Letters*, *39*, L20702. https://doi.org/10.1029/2012GL053409

Ashok, K., Behera, S. K., Rao, S. A., Weng, H., & Yamagata, T. (2007). El Niño Modoki and its possible teleconnection. *Journal of Geophysical Research*, *112*, C11007. https://doi.org/10.1029/2006JC003798

Ashok, S., Iizuka, S., Rao, A., Saji, N. H., & Lee, W.-J. (2009). Processes and boreal summer impacts of the 2004 El Nino Modoki. *Geophysical Research Letters*, *36*, L04703. https://doi.org/10.1029/2008GL036313

Baggett, C., & Lee, S. (2015). Arctic warming induced by tropically forced tapping of available potential energy and the role of the planetary-scale waves. *Journal of the Atmospheric Sciences*, *72*, 1562–1568. https://doi.org/10.1175/JAS-D-14-0334.1

Barnard, P., Allan, J., Hansen, J. E., Kaminsky, G. M., Ruggiero, P., & Doria, A. (2011). The impact of the 2009–10 El Nino Modoki on US west coast beaches. *Geophysical Research Letters*, *38*, L13604. https://doi.org/10.1029/2011GL047707

Barnard, P. L., Short, A. D., Harley, M. D., Splinter, K. D., Vitousek, S., Turner, I. L., … Heathfield, D. K. (2015). Coastal vulnerability across the Pacific dominated by El Niño/Southern Oscillation. *Nature Geoscience*, *8*(10), 801–807. https://doi.org/10.1038/ngeo2539

Barsugli, J. J., & Sardeshmukh, P. D. (2002). Global atmospheric sensitivity to tropical SST anomalies throughout the Indo-Pacific basin. *Journal of Climate*, *15*, 3427–3442.
Bellenger, H., Guilyardi, E., Leloup, J., Lengaigne, M., & Vialard, J. (2013). ENSO representation in climate models: From CMIP3 to CMIP5. *Climate Dynamics*, *42*(7–8), 1999–2018.
Bellucci, A., Gualdi, S., & Navarra, A. (2010). The double-ITCZ syndrome in coupled general circulation models: the role of large-scale vertical circulation regimes. *Journal of Climate*, *23*, 1127–1145.
Bjerknes, J. (1969). Atmospheric teleconnections from the equatorial pacific. *Monthly Weather Review*, *97*, 163–172.
Branstator, G., & Selten, F. (2009). Modes of variability and climate change. *Journal of Climate*, *22*, 2639–2658.
Brönnimann, S. (2007). Impact of El Niño–Southern Oscillation on European climate. *Reviews of Geophysics*, *45*, RG3003. https://doi.org/10.1029/2006RG000199
Butler, A. H., Polvani, L. M., & Deser, C. (2014). Separating the stratospheric and tropospheric pathways of El Niño–Southern Oscillation teleconnection. *Environmental Research Letters*, *9*, 024014. https://doi.org/10.1088/1748-9326/9/2/024014
Cai, W., Borlace, S., Lengaigne, M., van Rensch, P., Collins, M., Vecchi, G., … Jin, F. F. (2014). Increasing frequency of extreme El Niño events due to greenhouse warming. *Nature Climate Change*, *4*, 111–116. https://doi.org/10.1038/NCLIMATE2100
Cai, W., & Cowan, T. (2009). La Nina Modoki impacts Australia autumn rainfall variability. *Geophysical Research Letters*, *36*, L12805. https://doi.org/10.1029/2009GL037885
Cai, W., Santoso, A., Wang, G., Yeh, S. W., An, S. I., Cobb, K. M., … Wu, L. (2015). ENSO and greenhouse warming. *Nature Climate Change*, *5*(9), 849–859. https://doi.org/10.1038/NCLIMATE2743
Cai, W., & van Rensch, P. (2012). The 2011 southeast Queensland extreme summer rainfall: A confirmation of a negative Pacific Decadal Oscillation phase? *Geophysical Research Letters*, *39*, L08702. https://doi.org/10.1029/2011GL050820
Cai, W., van Rensch, P., Cowan, T., & Hendon, H. H. (2011). Teleconnection pathways of ENSO and the IOD and the mechanisms for impacts on Australian rainfall. *Journal of Climate*, *24*, 3910.
Cai, W., van Rensch, P., Cowan, T., & Hendon, H. H. (2012). An asymmetry in the IOD and ENSO teleconnection pathway and its impact on Australian climate. *Journal of Climate*, *25*, 6318–6329.
Cai, W., Wang, G., Santoso, A., McPhaden, M. J., Wu, L., Jin, F. F., … Guilyardi, E. (2015). Increased frequency of extreme La Niña events under greenhouse warming. *Nature Climate Change*, *5*(2), 132–137 https://doi.org/10.1038/NCLIMATE2492
Capotondi, A., Wittenberg, A. T., Newman, M., di Lorenzo, E., Yu, J. Y., Braconnot, P., … Yeh, S. W. (2015). Understanding ENSO diversity. *Bulletin of the American Meteorological Society*, *96*(6), 921–938, https://doi.org/10.1175/BAMS-D-13-00117.1.
Chadwick, R., Boutle, I., & Martin, G. (2013). Spatial patterns of precipitation change in CMIP5: Why the rich do not get richer in the tropics? *Journal of Climate*, *26*, 3803–3822.
Chiodi, A. M., & Harrison, D. E. (2013). El Niño impacts on seasonal U.S. atmospheric circulation, temperature, and precipitation anomalies: The OLR-event perspective. *Journal of Climate*, *23*(3), 822–837. https://doi.org/10.1175/JCLI-D-12-00097.1
Chiodi, A. M., & Harrison, D. E. (2015). Global seasonal precipitation anomalies robustly associated with El Niño and La Niña events—An OLR perspective. *Journal of Climate*, *28*, 6133–6159. https://doi.org/10.1175/JCLI-D-14-00387.1
Christensen, J. H., Krishna Kumar, K., Aldrian, E., An, S.-I., Cavalcanti, I. F. A., de Castro, M., … Zhou, T. (2013). Climate phenomena and their relevance for future regional climate change. In T. F. Stocker, et al. (Eds.), *Climate change 2013: The physical science basis. Contribution of Working Group I to the Fifth Assessment Report of the Intergovernmental Panel on Climate Change* (pp. 1217–1308). Cambridge, United Kingdom and New York: Cambridge Univeristy Press.
Clarke, A., & van Gorder, S. (1994). On ENSO coastal currents and sea levels. *Journal of Physical Oceanography*, *24*(3), 661–680.
Collins, M., An, S. I., Cai, W., Ganachaud, A., Guilyardi, E., Jin, F. F., … Wittenberg, A. (2010). The impact of global warming on the tropical Pacific Ocean and El Niño. *Nature Geoscience*, *3*(6), 391–397. https://doi.org/10.1038/ngeo868
Deser, C. (2000). On the teleconnectivity of the Arctic Oscillation. *Geophysical Research Letters*, *27*, 779–782.
Deser, C., Alexander, M. A., Xie, S.-P., & Phillips, A. S. (2010). Sea surface temperature variability: patterns and mechanism. *Annual Review of Marine Science*, *2*, 115–143.
Diaz, H. F., Hoerling, M. P., & Eischeid, J. K. (2001). ENSO variability, teleconnections and climate change. *International Journal of Climatology*, *21*, 1845–1862.
Ding, Q., Wallace, J. M., Battisti, D. S., Steig, E. J., Gallant, A. J., Kim, H. J., & Geng, L. (2014). Tropical forcing of the recentrapid Arctic warming in northeastern Canada and Greenland. *Nature*, *509*, 209–212. https://doi.org/10.1038/nature13260
Ding, Q.-H., Wang, B., Wallace, J. M., & Branstator, G. (2011). Tropical–extratropical teleconnections in boreal summer: Observed interannual variability. *Journal of Climate*, *24*, 1878–1896.
Dommenget, D., & Yu, Y. (2017). The effects of remote SST forcings on ENSO dynamics, variability and diversity. *Climate Dynamics*. https://doi.org/10.1007/s00382-016-3472-1
Enfield, D. B., Mestas-Nuñez, A. M., & Trimble, P. J. (2001). The Atlantic Multidecadal Oscillation and its relation to rainfall and river flows in the continental U.S. *Geophysical Research Letters*, *28*, 2077–2080. https://doi.org/10.1029/2000GL012745
England, M. H., & Huang, F. (2005). On the interannual variability of the Indonesian Throughflow and its linkage with ENSO. *Journal of Climate*, *18*, 1435–1444.
Fedorov, A. V., & Philander, S. G. (2000). Is El Niño changing? *Science*, *288*, 1997–2002.
Feng, M., McPhaden, M. J., Xie, S.-P., & Hafner, J. (2013). La Niña forces unprecedented Leeuwin Current warming in 2011. *Nature Science Reports*, *3*, 1277. https://doi.org/10.1038/srep01277
Folland, C. K., Renwick, J. A., Salinger, M. J., & Mullan, A. B. (2002). Relative influences of the Interdecadal Pacific Oscillation and ENSO on the South Pacific Convergence Zone. *Geophysical Research Letters*, *29*(13), 1643. https://doi.org/10.1029/2001GL014201
Fuentes-Franco, R., Giorgi, F., Coppola, E., & Kucharski, F. (2016) The role of ENSO and PDO in variability of winter precipitation over North America from twenty first century CMIP5 projections. *Climate Dynamics*, *46*, 3259–3277. https://doi.org/10.1007/s00382-015-2767-y
Frauen, C., Dommenget, D., Rezny, M., & Wales, S. (2014). Analysis of the non-linearity of El Niño Southern Oscillation teleconnections. *Journal of Climate*, *27*, 6225–6244.
Frischknecht, M., Münnich, M., & Gruber, N. (2015). Remote versus local influence of ENSO on the California Current System. *Journal of Geophysical Research: Oceans*, *120*, 1353–1374. https://doi.org/10.1002/2014JC010531
Garfinkel, C. I., Hurwitz, M. M., Waugh, D. W., & Butler, A. H. (2013). Are the teleconnections of Central Pacific and Eastern Pacific El Niño distinct in boreal wintertime? *Climate Dynamics*, *41*, 1835–1852.
Gershunov, A., & Barnett, T. P. (1998). Interdecadal modulation of ENSO teleconnections. *Bulletin of the American Meteorological Society*, *79*, 2715–2272.

Giannini, A., Chiang, J. C. H., Cane, M. A., Kushnir, Y., & Seager, R. (2001). The ENSO teleconnection to the tropical Atlantic ocean: Contributions of the remote and local SSTs to rainfall variability in the tropical Americas. *Journal of Climate*, *14*, 4530–4544.
Giannini, A., Kushnir, Y., & Cann, M. A. (2000). Interannual variability of Caribbean rainfall, ENSO and the Atlantic Ocean. *Journal of Climate*, *13*, 297–311.
Giese, B. S.,& Ray, S. (2011). El Niño variability in simple ocean data assimilation (SODA), 1871–2008. *Journal of Geophysical Research*, *116*, C02024. https://doi.org/10.1029/2010JC006695
Gill, A. E. (1980). Some simple solutions for heat-induced tropical circulation. *Quarterly Journal of the Royal Meteorological Society*, *106*, 447–462.
Gordon, A. L., & Fine, R. A. (1996). Pathways of water between the Pacific and Indian oceans in the Indonesian seas. *Nature*, *379*, 146–149.
Graf, H.-F., & Zanchettin, D. (2012). Central Pacific El Niño, the "subtropical bridge," and Eurasian climate. *Journal of Geophysical Research*, *117*, D01102. https://doi.org/10.1029/2011JD016493
Graham, N. E. (1994). Decadal-scale climate variability in the 1970s and 1980s: Observations and model results. *Climate Dynamics*, *10*, 135–162.
Guilyardi, E., Gualdi, S., Slingo, J., Navarra, A., Delecluse, P., Cole, J., … Terray, L. (2004). Representing El Niño in coupled ocean–atmosphere GCMs: The dominant role of the atmospheric component. *Journal of Climate*, *17*(24), 4623–4629. https://doi.org/10.1175/JCLI-3260.1
Guilyardi, E., Wittenberg, A., Fedorov, A., Collins, M., Wang, C. Z., Capotondi, A., … Stockdale, T. (2009). Understanding El Nin˜o in ocean–atmosphere general circulation models: Progress and challenges. *Bulletin of the American Meteorological Society*, *90*, 325–340.
Gutierrez, D., Enriquez, E., Purca, S., Quipuzcoa, L., Marquina, R., Flores, G., & Graco, M. (2008). Oxygenation episodes on the continental shelf of central Peru: Remote forcing and benthic ecosystem response. *Progress in Oceanography*, *79*, 177–189.
Ha, K.-J., Chu, J.-E., Lee, J.-Y., & Yun, K.-S. (2016). Interbasin coupling between the tropical Indian and Pacific Ocean on interannual timescale: Observation and CMIP5 reproduction. *Climate Dynamics*. https://doi.org/10.1007/s00382-016-3087-6
Ham, Y. G., & Kug, J.-S. (2016). ENSO amplitude changes due to greenhouse warming in CMIP5: Role of mean tropical precipitation in the twentieth. *Geophysical Research Letters*, *43*, 422–430. https://doi.org/10.1002/2015GL066864
Ham, Y. G., Sung, M.-K., An, S.-I., Schubert, S. D., & Kug, J.-S. (2014). Role of tropical Atlantic SST variability as a modulator of El Niño teleconnections. *Asia-Pacific Journal of Atmospheric Sciences*, *50*, 247–261.
Han, W., Meehl, G., Hu, A., Alexander, M., Yamagata, T., Yuan, D., … Leben, R. (2014). Intensification of decadal and multi-decadal sea level variability in the western tropical Pacific during recent decades. *Climate Dynamics*, *43*, 1357–1379. https://doi.org/10.1007/s00382-013-1951-1
Handoh, I. C., Adrian, J. M., Grant, R. B., & David, P. S. (2006). Interannual variability of the tropical atlantic independent of and associated with ENSO: Part I. The North Tropical Atlantic. *International Journal of Climatology*, *26*(14), 1937–1956. https://doi.org/10.1002/joc.1343
Hazeleger, W., Seager, R., Cane, M. A., & Naik, N. H. (2004). How can tropical Pacific Ocean heat transport vary? *Journal of Physical Oceanography*, *34*, 320–333.
Held, I. M., & Soden, B. J. (2006). Robust responses of the hydrological cycle to global warming. *Journal of Climate*, *19*, 5686–5699.
Hong, C.-C., Wu, Y.-K., Li, T., & Chang, C.-C. (2014). The climate regime shift over the Pacific during 1996/1997. *Climate Dynamics*, *43*, 435–446.
Horel, J. D., & Wallace, J. M. (1981). Planetary-scale atmospheric phenomena associated with the Southern Oscillation. *Monthly Weather Review*, *109*, 813–829.
Hoskins, B. J., & Karoly, D. J. (1981). The steady linear response of a spherical atmosphere to thermal and orographic forcing. *Journal of the Atmospheric Sciences*, *38*, 1179–1196.
Hu, Z.-Z., & Huang, B. (2009). Interferential impact of ENSO and PDO on dry and wet conditions in the US Great Plains. *Journal of Climate*, *22*, 6047–6065.
Huang, B. (2004). Remotely forced variability in the tropical Atlantic Ocean. *Climate Dynamics*, *23*(2), 133–152.
Huang, P., & Xie, S.-P. (2015). Mechanisms of change in ENSO-induced tropical Pacific rainfall variability in a warming climate. *Nature Geoscience*, *8*(12), 922–926. https://doi.org/10.1038/NGEO2571
Ineson, S., & Scaife, A. A. (2009). The role of the stratosphere in the European climate response to El Niño. *Nature Geoscience*, *2*, 32–36. https://doi.org/10.1038/ngeo381
IPCC (2013). *Climate change 2013: The physical science basis: Working group I contribution to the fifth assessment report of the intergovernmental panel on climate change* (Vol. 1, pp. 1–1535). New York: Cambridge University Press. https://doi.org/10.1017/CBO9781107415324
Jin, F.-F., Boucharel, J., & Lin, I.-I. (2014). Eastern Pacific tropical cyclones intensified by El Niño delivery of subsrface ocean heat. *Nature*, *516*, 82–85.
Jo, H.-S., Yeh, S.-W., & Kim, C.-H. (2013). A possible mechanism for the North Pacific climate transitions of the winter of 1998/99. *Geophysical Research Letters*, *40*, 1–6.
Jo, H.-S., Yeh, S.-W., & Kirtman, B. P. (2014). Role of the western tropical Pacific in the North Pacific regime shift in the winter of 1998/99. *Journal of Geophysical Research*, *119*, 6161–6170. https://doi.org/10.1002/2013JC009527
Jo, H.-S., Yeh, S.-W., & Lee, S.-K. (2015). Changes in the relationship in the SST variability between the tropical Pacific and the North Pacific across the 1998/1999 regime shift. *Geophysical Research Letters*, *42*, 7171–7178. https://doi.org/10.1002/2015GL065049
Jong, B.-T., Ting, M., & Seager, R. (2016). El Niño's impact on California precipitation: Seasonality, regionality, and El Niño's intensity. *Environmental Research Letters*, *11*, 054021.
Kalnay, E., Kanamitsu, M., Kistler, R., Collins, W., Deaven, D., Gandin, L., … Joseph, D. (1996). The NCEP/NCAR 40-year reanalysis project. *Bulletin of the American Meteorological Society*, *77*(3), 437–471. https://doi.org/10.1175/1520-0477(1996)077%3C0437:TNYRP%3E2.0.CO;2
Kao, H.-Y., & Yu, J.-Y. (2009). Contrasting eastern-Pacific and central-Pacific types of ENSO. *Journal of Climate*, *22*, 615–632.
Karoly, D. J. (1989). Southern hemisphere circulation features associated with El Niño-Southern Oscillation events. *Journal of Climate*, *2*, 1239–1252.
Kenyon, J., & Hegerl, G. C. (2008). Influence of modes of climate variability on global temperature extremes. *Journal of Climate*, *21*, 3872–3889.
Kenyon, J., & Hegerl, G. C. (2010). Influence of modes of climate variability on global precipitation extremes. *Journal of Climate*, *23*, 6248–6262.
Kim, J., Yeh, S.-W., & Chang, E.-C. (2014). Combined effect of El Niño-Southern Oscillation and Pacific decadal oscillation on the East Asian winter monsoon. *Climate Dynamics*, *42*, 957–971.
Kim, S.-T., & Yu, J.-Y. (2009). The two types of ENSO in CMIP5 models. *Geophysical Research Letters*, *39*, L11704.
King, A. D., van Oldenborgh, G. J., & Karoly, D. J. (2016). Climate change and El Nino increase likelihood of Indonesian heat and drought. *Bulletin of the American Meteorological Society*, *97*, S113–S117.
Klein, S. A., Soden, B. J., & Lau, N.-C. (1999). Remote sea surface temperature variations during ENSO: Evidence for a tropical atmospheric bridge. *Journal of Climate*, *12*, 917–932.
Kosaka, Y., & Xie, S. P. (2013). Recent global-warming hiatus tied to equatorial Pacific surface cooling. *Nature*, *501*, 403–407.

Kug, J.-S., An, S.-I., Ham, Y.-G., & Kang, I.-S. (2009). Changes in El Niño and La Niña teleconnections over North Pacific–America in the global warming simulations. *Theoretical and Applied Climatology*, *100*, 275–282.
Kug, J.-S., Jin, F.-F., & An, S.-I. (2009). Two types of El Niño events: Cold tongue El Niño and warm pool El Niño. *Journal of Climate*, *22*, 1499–1515.
Kumar, A., & Chen, M. (2017). What is the variability in US west coast winter precipitation during strong El Nino events? *Climate Dynamics*. *49*(7-8), 2789–2802. https://doi.org/10.1007/s00382-016-3485-9
Kumar, A., & Hoerling, M. P. (2003). The nature and causes for the delayed atmospheric response to El Niño. *Journal of Climate*, *16*(9), 1391–1403.
Kumar, K. K., Rajagopalan, B., Hoerling, M., Bates, G., & Cane, M. (2006). Unraveling the mystery of Indian monsoon failure during El Niño. *Science*, *314*, 115–119.
Kumar, P., Min, S.-K., Weller, E., Lee, H., & Wang, X. L. (2016). Influence of climate variability on extreme ocean surface wave heights assessed from ERA-Interim and ERA-20C reanalyses. *Journal of Climate*, *29*, 4031–4046.
Kwok, R., Comiso, J. C., Lee, T., & Holland, P. R. (2016). Linked trends in the South Pacific sea ice edge and Southern Oscillation Index. *Geophysical Research Letters*, *43*, 10,295–10,302. https://doi.org/10.1002/2016GL070655
Langenbrunner, B., & Neelin, J. D. (2013). Analyzing ENSO teleconnections in CMIP models as a measure of model fidelity in simulating precipitation. *Journal of Climate*, *26*, 4431–4446.
Lau, N. C. (1997). Interactions between global SST anomalies and the midlatitude atmospheric circulation. *Bulletin of the American Meteorological Society*, *78*, 21–33.
Lee, T., & McPhaden, M. J. (2010). Increasing intensity of El Niño in the central-equatorial Pacific. *Geophysical Research Letters*, *37*, L14603. https://doi.org/10.1029/2010GL044007
Li, G., & Xie, S.-P. (2014). Tropical biases in CMIP5 multimodel ensemble: The excessive equatorial Pacific cold tongue and double ITCZ problems. *Journal of Climate*, *27*, 1765–1780.
Lin, J. L. (2007). The double-ITCZ problem in IPCC AR4 coupled GCMs: Ocean–atmosphere feedback analysis. *Journal of Climate*, *20*, 4497–4525.
Liu, W., Huang, B., Thorne, P. W., Banzon, V. F., Zhang, H.-M., Freeman, E., … Woodruff, S. D. (2014). Extended Reconstructed Sea Surface Temperature version 4 (ERSST.v4): Part II. Parametric and structural uncertainty estimations. *Journal of Climate*, *28*, 931–951.
Lloyd, J., Guilyardi, E., & Weller, H. (2011). The role of atmosphere feedbacks during ENSO in the CMIP3 models. Part II: Using AMIP runs to understand the heat flux feedback mechanisms. *Climate Dynamics*, *37*, 1271–1292.
Lyon, L. B., Barnston, G. A., & Dewitt, D. G. (2014). Tropical Pacific forcing of a 1998–1999 climate shift: Observational analysis and climate model results for the boreal spring speason. *Climate Dynamics*, *43*, 893–909.
Mantua, N. J., Hare, S. R., Zhang, Y., Wallace, J. M., & Francis, R. C. (1997). A Pacific interdecadal climate oscillation with impacts on salmon production. *Bulletin of the American Meteorological Society*, *78*, 1069–1079.
Marathe, S., Ashok, K., Swapna, P., & Sabin, T. P. (2015). Revisiting El Nino Modoki. *Climate Dynamics*, *45*, 3527–3545.
Matsuno, T. (1966). Quasi-geostrophic motions in the equatorial area. *Journal of the Meteorological Society of Japan*, *44*, 25–43.
McPhaden, M. J. (2004). Evolution of the 2002/2003 El Nino. *Bulletin of the American Meteorological Society*, *85*(5), 677–695. https://doi.org/10.1175/BAMS-85-5-677
McPhaden, M. J. (2012). A 21st century shift in the relationship between ENSO SST and warm water volume anomalies. *Geophysical Research Letters*, *39*, L09706. https://doi.org/10.1029/2012GL051826
McPhaden, M. J., Lee, T., & McClurg, D. (2011). El Niño and its relationship to changing background conditions in the tropical Pacific Ocean. *Geophysical Research Letters*, *38*, L15709. https://doi.org/10.1029/2011GL048275
McPhaden, M. J., Zebiak, S. E., & Glantz, M. H. (2006). ENSO as an integrating concept in earth science. *Science*, *314*, 1740–1745.
Medhaug, I., Stolpe, M. B., Fischer, E. M., & Knutti, R. (2017). Reconciling controversies about the global warming hiatus. *Nature*, *545*, 41–47.
Meehl, G. A., Arblaster, J. M., & Chung, C. T. Y. (2015). Disappearance of the southeast U.S. "warming hole" with the late-1990s transition of the Interdecadal Pacific Oscillation. *Geophysical Research Letters*, *42*, 5564–5570. https://doi.org/10.1002/2015GL064586
Meehl, G. A., Arblaster, J. M., Fasullo, J. T., Hu, A., & Trenberth, K. E. (2011). Model-based evidence of deep-ocean heat uptake during surface-temperature hiatus periods. *Nature Climate Change*, *1*(7), 360–364. https://doi.org/10.1038/nclimate1229
Meehl, G. A., & Hu, A. (2006). Megadroughts in the Indian monsoon region and southwest North America and a mechanism for associated multidecadal Pacific sea surface temperature anomalie. *Journal of Climate*, *19*, 1605–1623.
Meehl, G. A., Stocker, T. F., Collins, W. D., Friedlingstein, P., Gaye, A. T., Gregory, J. M., … Zhao, Z.-C. (2007). Global Climate Projections. In S. Solomon, et al. (Eds.), *Climate change 2007: The physical science basis. Contribution of working group I to the 4th assessment report of the intergovernmental panel on climate change* (747–845). Cambridge, United Kingdom and New York: Cambridge University Press.
Meehl, G. A., Tebaldi, C., Teng, H., & Peterson, T. C. (2007). Current and future US weather extremes and El Niño. *Geophysical Research Letters*, *34*, L20704. https://doi.org/10.1029/2007GL031027
Meehl, G. A., & Teng, H. (2007). Multi-model changes in El Niño teleconnections over North America in a future warmer climate. *Climate Dynamics*. https://doi.org/10.1007/s00382-007-0268-3
Meehl, G. A., Teng, H., & Arblaster, J. M. (2014). Climate model simulations of the observed early-2000s hiatus of global warming. *Nature Climate Change*, *4*, 898–902. https://doi.org/10.1038/NCLIMATE2357
Meyers, S. D., Melsom, A., Mitchum, G. T., & O'Brien, J. J. (1998). Detection of the fast Kelvin wave teleconnection due to El Niño-Southern Oscillation. *Journal of Geophysical Research*, *103*, 27,655–27,663.
Min, S.-K., Cai, W., & Whetton, P. (2013). Influence of climate variability on seasonal extremes over Australia. *Journal of Geophysical Research*, *118*, 643–654.
Mo, K. C. (2010). Relationships between low-frequency variability in the Southern Hemisphere and sea surface temperature anomalies. *Journal of Climate*, *13*, 3599–3610.
Müller, W. A., & Roeckner, E. (2008). ENSO teleconnections in projections of future climate in ECHAM5/MPI-OM. *Climate Dynamics*, *31*, 533–549.
Newman, M., Alexander, M. A., Ault, T. R., Cobb, K. M., Deser, C., di Lorenzo, E., … Smith, C. A. (2016). The Pacific Decadal Oscillation, Revisited. *Journal of Climate*, *29*(12), 4399–4427. https://doi.org/10.1175/JCLI-D-15-0508.1
Newman, M., Shin, S.-I., & Alexander, M. A. (2011). Natural variation in ENSO flavors. *Geophysical Research Letters*, *38*, L14705. https://doi.org/10.1029/2011GL047658
Nicholls, N. (1989). Sea surface temperatures and Australian winter rainfall. *Journal of Climate*, *2*, 965–973.
Nicolas, J. P., Vogelmann, A. M., Scott, R. C., Wilson, A. B., Cadeddu, M. P., Bromwich, D. H., … Wille, J. D. (2017). January 2016 extensive summer melt in West Antarctica favored by strong El Nino. *Nature Communications*. *8*. https://doi.org/10.1038/ncomms15799

Okumura, Y., Xie, S. P., Numaguti, A., & Tanimoto, Y. (2001). Tropical Atlantic air-sea interaction and its influence on the NAO. *Geophysical Research Letters*, *28*, 1507–1510. https://doi.org/10.1029/2000GL012565

Okumura, Y. M., Ohba, M., Deser, C., & Ueda, H. (2011). A proposed mechanism for the asymmetric duration of El Niño and La Niña. *Journal of Climate*, *24*, 3822–3829.

Pavia, E. G., Graef, F., & Reyes, J. (2006). PDO–ENSO effects in the climate of Mexico. *Journal of Climate*, *19*(24), 6433–6438.

Pineda, L., Ntegeka, V., & Willems, P. (2013). Rainfall variability related to sea surface temperature anomalies in a Pacific–Andean basin into Ecuador and Peru. *Advances in Geosciences*, *33*, 53–62.

Pope, J. O., Holland, P. R., Orr, A., Marshall, G. J., & Phillips, T. (2017). The impacts of El Niño on the observed sea ice budget of West Antarctica. *Geophysical Research Letters*, *44*, 6200–6208. https://doi.org/10.1002/2017GL073414

Power, S., Casey, T., Folland, C., Colman, A., & Mehta, V. (1999). Inter-decadal modulation of the impact of ENSO on Australia. *Climate Dynamics*, *15*, 319–324.

Power, S., Delage, F., Chung, C., Kociuba, G., & Keay, K. (2013). Robust twenty-first-century projections of El Niño and related precipitation variability. *Nature*, *502*, 541–545.

Preethi, B., Sabin, T. P., Adedoyin, J. A., & Ashok, K. (2015). Impacts of the ENSO Modoki and other tropical Indo-Pacific climate-drivers on African rainfall. *Nature Science Report*, *5*, 16653.

Rasmusson, E. M., & Carpenter, T. H. (1983). The relationship between eastern equatorial Pacific sea surface temperatures and rainfall over India and Sri Lanka. *Monthly Weather Review*, *111*, 517–528.

Richter, I. (2015). Climate model biases in the eastern tropical oceans: Causes, impacts and ways forward. *WIREs Climate Change*, *6*, 345–358.

Risbey, J. S., & Lewandowsky, S. (2017). The 'pause' unpacked. *Nature*, *545*, 37–38.

Rodrigues, R. R., Haarsma, R. J., Campos, E. J. D., & Ambrizzi, T. (2011). The impacts of inter-El Niño variability on the Tropical Atlantic and Northeast Brazil climate. *Journal of Climate*, *24*, 3402–3422.

Rodrigues, R. R., & McPhaden, M. J. (2014). Why did the 2011–2012 La Nina cause a severe drought in the Brazilian Northeast? *Geophysical Research Letters*, *41*, 1012–1018. https://doi.org/10.1002/2013GL058703

Saji, N. H., Goswami, B. N., Vinayachandran, P. N., & Yamagata, T. (1999). A dipole mode in the tropical Indian Ocean. *Nature*, *401*, 360–363.

Saji, N. H., & Yamagata, T. (2003). Possible impacts of Indian Ocean dipole mode events on global climate. *Climate Research*, *25*, 151–169.

Schemm, S., Ciasto, L. M., Li, C., & Kvamstø, N. G. (2016). Influence of tropical Pacific Sea surface temperature on the genesis of gulf stream cyclones. *Journal of the Atmospheric Sciences*, *73*, 4203–4214. https://doi.org/10.1175/JAS-D-16-0072.1

Schneider, E. K., Fennessy, M. J., & Kinter, J. L. III (2009). A statistical-dynamical estimate of winter ENSO teleconnections in a future climate. *Journal of Climate*, *22*, 6624–6638.

Schneider, N., & Cornuelle, B. D. (2005). The forcing of the Pacific Decadal Oscillation. *Journal of Climate*, *18*, 4355–4377.

Seager, R., Naik, N., & Vogel, L. (2012). Does global warming cause intensified interannual hydroclimate variability? *Journal of Climate*, *25*, 3355–3372.

Sikka, D. R. (1980). Some aspects of the large scale fluctuations of summer monsoon rainfall over India in relation to fluctuations in the planetary and regional scale circulation parameters. *Proceedings of the Indian Academy of Science*, *89*(2), 179–195.

Song, H.-J., Choi, E., Lim, G.-H., Kim, Y. H., Kug, J.-S., & Yeh, S.-W. (2011). The central Pacific as the export region of the El Niño-Southern Oscillation sea surface temperature anomaly to Antarctica sea ice. *Journal of Geophysical Research*, *116*, D21113. https://doi.org/10.1029/2011JD015645

Stan, C., Straus, D. M., Frederiksen, J. S., Lin, H., Maloney, E. D., & Schumacher, C. (2017). Review of tropical-extratropical teleconnections on intraseasonal time scales. *Reviews of Geophysics*, *55*. https://doi.org/10.1002/2016RG000538

Stevenson, S., Fox-Kemper, B., Jochum, M., Rajagopalan, B., & Yeager, S. G. (2010). ENSO model validation using wavelet probability analysis. *Journal of Climate*, *23*(20), 5540–5547.

Stevenson, S. L. (2012). Significant changes to ENSO strength and impacts in the twenty-first century: Results from CMIP5. *Geophysical Research Letters*, *39*, L17703. https://doi.org/10.1029/2012GL052759

Sun, X., Greatbatch, R. J., Park, W., & Latif, M. (2011). Two major modes of variability of the East Asian summer monsoon. *Quarterly Journal of the Royal Meteorological Society*, *136*, 829–841.

Sung, M.-K., Ham, Y. G., Kug, J.-S., & An, S.-I. (2013). An alternative effect by the tropical North Atlantic SST in intraseasonally varying El Niño teleconnection over the North Atlantic. *Tellus A*, *65*, 19863.

Suppiah, R. (2004). Trends in the southern oscillation phenomenon and Australian rainfall and changes in their relationship. *International Journal of Climatology*, *24*, 269–290. https://doi.org/10.1002/joc.1001

Takahashi, K., Montecinos, A., Goubanova, K., & Dewitte, B. (2011). ENSO regimes: reinterpreting the canonical and Modoki El Niño. *Geophysical Research Letters*, *38*, L10704. https://doi.org/10.1029/2011GL047364

Tao, W., Huang, G., Hu, K., Qu, X., Wen, G., & Gong, H. (2015). Interdecadal modulation of ENSO teleconnections to the Indian Ocean Basin Mode and their relationship under global warming in CMIP5 models. *International Journal of Climatology*. https://doi.org/10.1002/joc.3987

Taschetto, A. S., & England, M. H. (2009). El Niño Modoki impacts on Australian rainfall. *Journal of Climate*, *22*, 3167–3174.

Taschetto, A. S. R., Rodrigues, R., Meehl, G. A., McGregor, S., & England, M. H. (2016). How sensitive are the Pacific-North Atlantic teleconnections to the position and intensity of El Niño-related warming. *Climate Dynamics*, *46*, 1841–1860.

Thompson, D. W., & Wallace, J. M. (1998). The Arctic Oscillation signature in the wintertime geopotential height and temperature fields. *Geophysical Research Letters*, *25*, 1297–1300. https://doi.org/10.1029/98GL00950

Trenberth, K. E., Branstator, G. W., Karoly, D., Kumar, A., Lau, N. C., & Ropelewski, C. (1998). Progress during TOGA in understanding and modeling global teleconnections associated with tropical sea surface temperatures. *Journal of Geophysical Research*, *103*, 14,291–14,324. https://doi.org/10.1029/97JC01444

Trenberth, K. E., Dai, A., Schrier, G. V., Jones, P. D., Barichivich, J., Briffa, K. R., & Sheffield, J. (2014). Global warming and changes in drought. *Nature Climate Change*, *4*, 17–22.

Trenberth, K. E., & Hurrell, J. W. (1994). Decadal atmospheric-ocean variations in the Pacific. *Climate Dynamics*, *9*, 303–309.

Trenberth, K. E., & Stepaniak, D. P. (2001). Indices of El Niño evolution. *Journal of Climate*, *14*, 1697–1701.

Turner, J. (2004). The El-Niño-Southern Oscillation and Antarctica. *International Journal of Climatology*, *24*, 1–31. https://doi.org/10.1002/joc.965

Van Oldenborgh, G. J., & Burgers, G. (2005). Searching for decadal variations in ENSO precipitation teleconnections. *Geophysical Research Letters*, *32*, L15701. https://doi.org/10.1029/2005GL023110

Vecchi, G. A., & Soden, B. J. (2007). Global warming and the weakening of the tropical circulation. *Journal of Climate*, *20*, 4316–4340.

Vecchi, G. A., & Wittenberg, A. T. (2010). El Niño and our future climate: Where do we stand? *Wiley Interdisciplinary Reviews: Climate Change*, *1*, 260–270.

Vergara, O., Dewitte, B., Ramos, M., & Pizarro, O. (2017). Vertical energy flux at ENSO time scales in the subthermocline of the Southeastern Pacific. *Journal of Geophysical Research: Oceans*, *122*, 6011–6038. https://doi.org/10.1002/2016JC012614

Wang, B., & An, S.-I. (2002). A mechanism for decadal changes of ENSO behavior: Roles of background wind changes. *Climate Dynamics*, *18*, 475–486.

Wang, C. (2002). Atmospheric circulation cells associated with the El Niño-Southern Oscillation. *Journal of Climate*, *15*, 399–419.

Wang, G., Cai, W., Gan, B., Wu, L., Santose, A., Lin, X., … McPhaden, M. J. (2017). Continued increase of extreme El Niño frequency long after 1.5°C warming stabilization. *Nature Climate Change*. https://doi.org/10.1038/NCLIMATE3351

Wang, G., & Hendon, H. H. (2007). Sensitivity of Australian rainfall to inter-El Niño variations. *Journal of Climate*, *20*, 4211–4226.

Watanabe, M., Kug, J.-S., Jin, F.-F., Collins, M., Ohba, M., & Wittenberg, A. T. (2012). Uncertainty in the ENSO amplitude change from the past to the future. *Geophysical Research Letters*, *39*, L20703. https://doi.org/10.1029/2012GL053305

Webster, P. J., Magana, V., Palmer, T. N., Shukla, J., Tomas, R. A., Yanai, M., & Yasunari, T. (1998). Monsoons: Processes, predictability and the prospects for prediction. *Journal of Geophysical Research*, *103*, 14,451–14,510.

Webster, P. J., Moore, A. M., Loschnigg, J. P., & Leben, R. R. (1999). Coupled ocean-atmosphere dynamics in the Indian Ocean during 1997-98. *Nature*, *401*, 356–360.

Wei, W., Zhang, R., Wen, M., Rong, X., & Li, T. (2014). Impact of Indian summer monsoon on the South Asian High and its influence on summer rainfall over China. *Climate Dynamics*, *43*, 1257–1269.

Weng, H., Ashok, K., Behera, S. K., Rao, S. A., & Yamagata, T. (2007). Impacts of recent El Niño Modoki on dry/wet conditions in the Pacific rim during boreal summer. *Climate Dynamics*, *29*, 113–129.

Wilson, A. B., Bromwich, D. H., Hines, K. M., & Wang, S.-H. (2014). El Nino flavors and their simulated impacts on atmospheric circulation in the high southern latitudes. *Journal of Climate*, *27*, 8934–8955.

Wittenberg, A. T. (2009). Are historical records sufficient to constrain ENSO simulations? *Geophysical Research Letters*, *36*, L12306. https://doi.org/10.1029/2009GL038710

Xiang, B., Wang, B., & Li, T. (2013). A new paradigm for the predominance of standing Central Pacific Warming after the late 1990s. *Climate Dynamics*, *41*, 327–340.

Xie, S.-P., Kosaka, Y., Du, Y., Hu, K., Chowdary, J., & Huang, G. (2016). Indo-western Pacific ocean capacitor and coherent climate anomalies in post-ENSO summer: A review. *Advances in Atmospheric Sciences*, *33*, 411–432.

Xie, S. P., & Philander, S. G. H. (1994). A coupled ocean–atmosphere model of relevance to the ITCZ in the eastern Pacific. *Tellus*, *46*, 340–350.

Yang, J., Liu, Q., Xi, S.-P., Liu, Z., & Wu, L. (2007). Impact of the Indian Ocean basin mode on the Asian summer monsoon. *Geophysical Research Letters*, *34*, L02708. https://doi.org/10.1029/2006GL028571

Yeh, S.-W., Kirtman, B. P., Kug, J.-S., Park, W., & Latif, M. (2011). Natural variability of the central Pacific El Niño event on multi-centennial timescales. *Geophysical Research Letters*, *38*, L02704. https://doi.org/10.1029/2010GL045886

Yeh, S.-W., Kug, J.-S., & An, S.-I. (2014). Recent progress on two types of El Niño: Observations, dynamics, and future changes. *Asia-Pacific Journal of Atmospheric Sciences*, *50*(1), 69–81.

Yeh, S.-W., Kug, J.-S., Dewitte, B., Kwon, M.-H., Kirtman, B. P., & Jin, F.-F. (2009). El Niño in a changing climate. *Nature*, *461*, 511–514.

Yeh, S.-W., Wang, X., Wang, C., & Dewitte, B. (2015). On the relationship between the North Pacific climate variability and the Central Pacific El Niño. *Journal of Climate*, *28*, 663–677.

Yu, J.-Y., & Zou, Y. (2013). The enhanced drying effect of Central-Pacific El Niño on US winter. *Environmental Research Letters*, *8*. https://doi.org/10.1088/1748-9326/8/1/014019

Zhang, Y., Wallace, J. M., & Battisti, D. S. (1997). ENSO-like interdecadal variability: 1900–93. *Journal of Climate*, *10*, 1004–1020.

Zheng, X.-T., Xie, S.-P., Lv, L.-H., & Z-Qm, Z. (2016). Intermodel uncertainty in ENSO amplitude change tied to Pacific ocean warming pattern. *Journal of Climate*, *29*, 7265–7279.

Zhou, Z.-Q., Xie, S.-P., Zheng, X.-T., Liu, Q., & Wang, H. (2014). Global warming–induced changes in El Niño teleconnections over the North Pacific and North America. *Journal of Climate*, *27*, 9050–9064.

Erratum

In the originally published version of this article, the reference and DOI for Schemm et al. were incorrect. It has since been replaced with the correct reference and DOI (https://doi.org/10.1175/JAS-D-16-0072.1) and this version may be considered the authoritative version of record.